GOBIERNO DE ESPAÑA
MINISTERIO DE CIENCIA, INNOVACIÓN Y UNIVERSIDADES
Ciemat
Centro de Investigaciones Energéticas, Medioambientales y Tecnológicas
EXCELENCIA MARÍA DE MAEZTU
cfp CIEMAT física de partículas

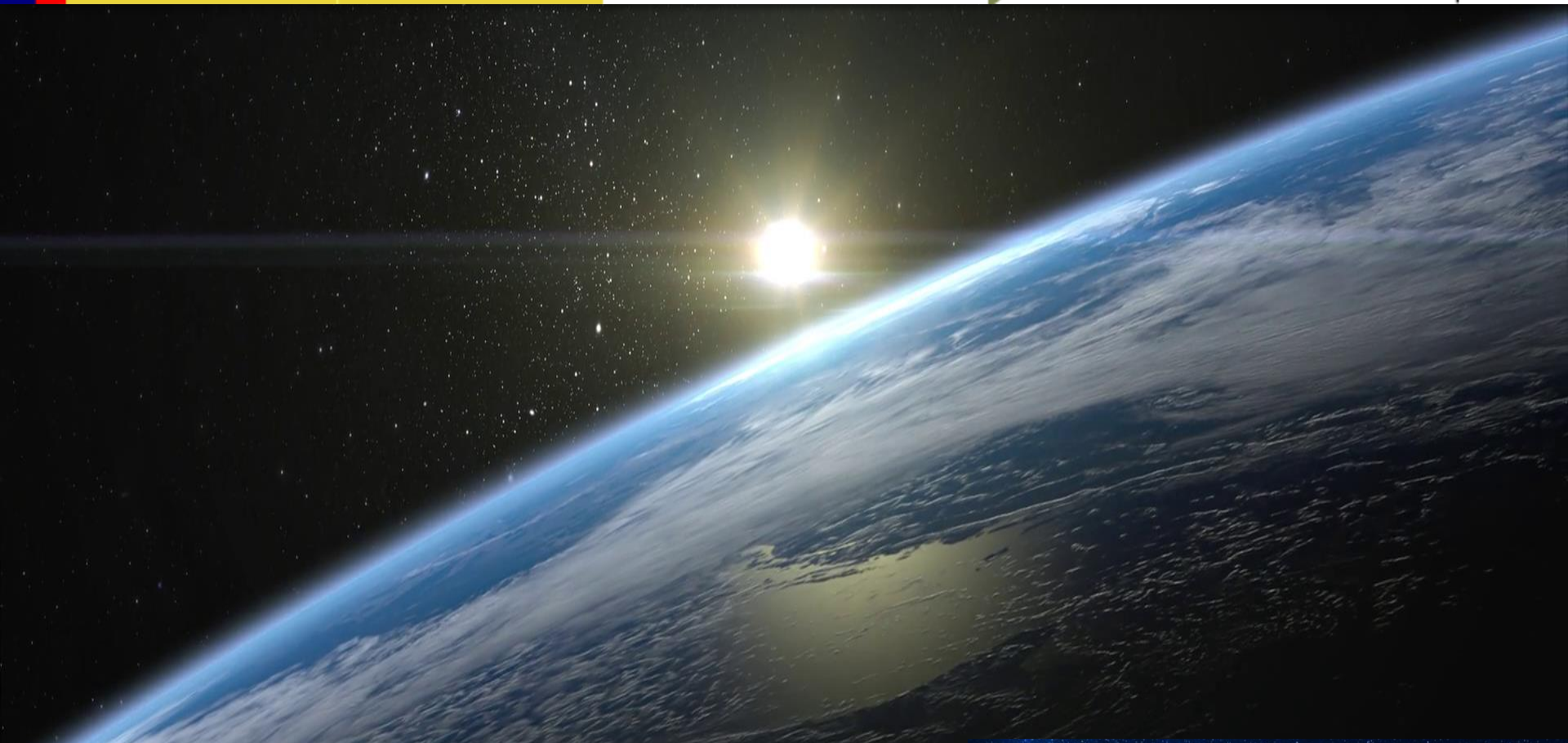

Cosmic Ray Anisotropies with space-based detectors

M. A. Velasco, CIEMAT, Madrid (Spain)

CRA2019
COSMIC RAY ANISOTROPY WORKSHOP
October 7th - 11th 2019
GSSI L'Aquila Italy

Cosmic Ray Spectrum

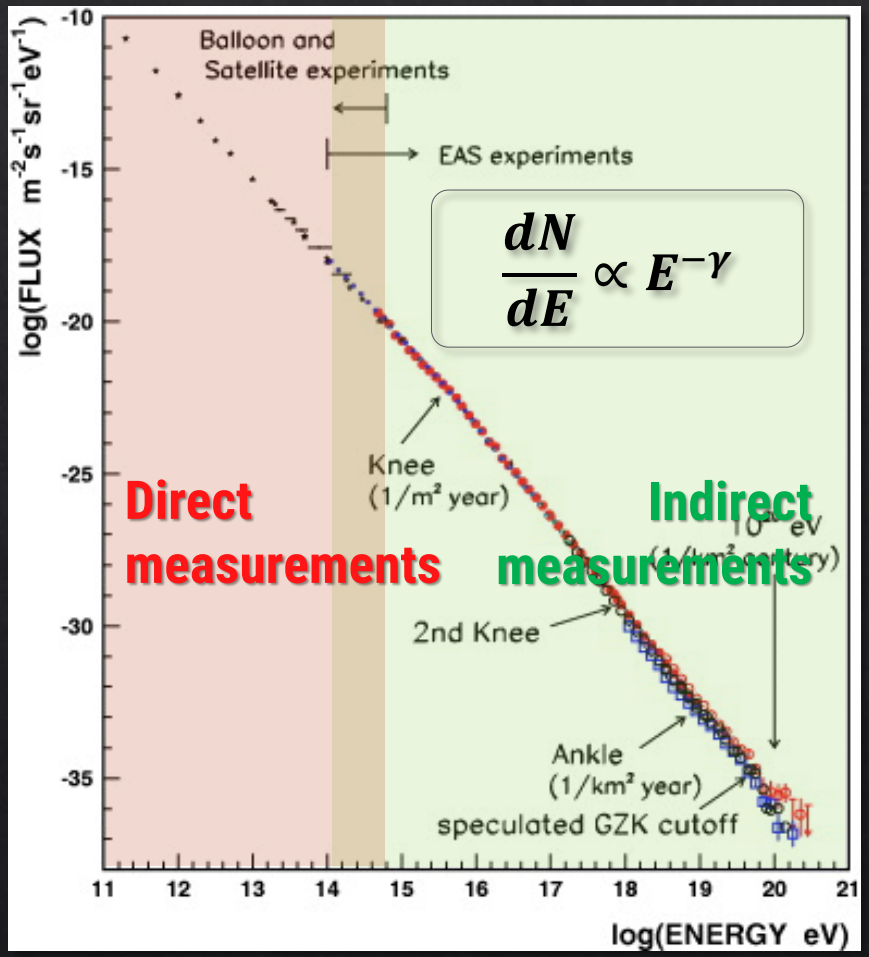

[M. Nagano, New J. Phys. **11** 065012 (2009)]

Direct measurements (space-based/balloon-borne)

☺ Particle identification

☹ Weight/size constrains: limits in the energy range

Indirect measurements (ground-based)

☺ Extended energy range

☹ Particle identification: dependence on models about atmospheric interactions

DIRECT & INDIRECT MEASUREMENTS PROVIDE COMPLEMENTARY INFORMATION

(Some) Open Questions in GCRs Physics

Cosmic Rays in the GeV – TeV range have a galactic origin

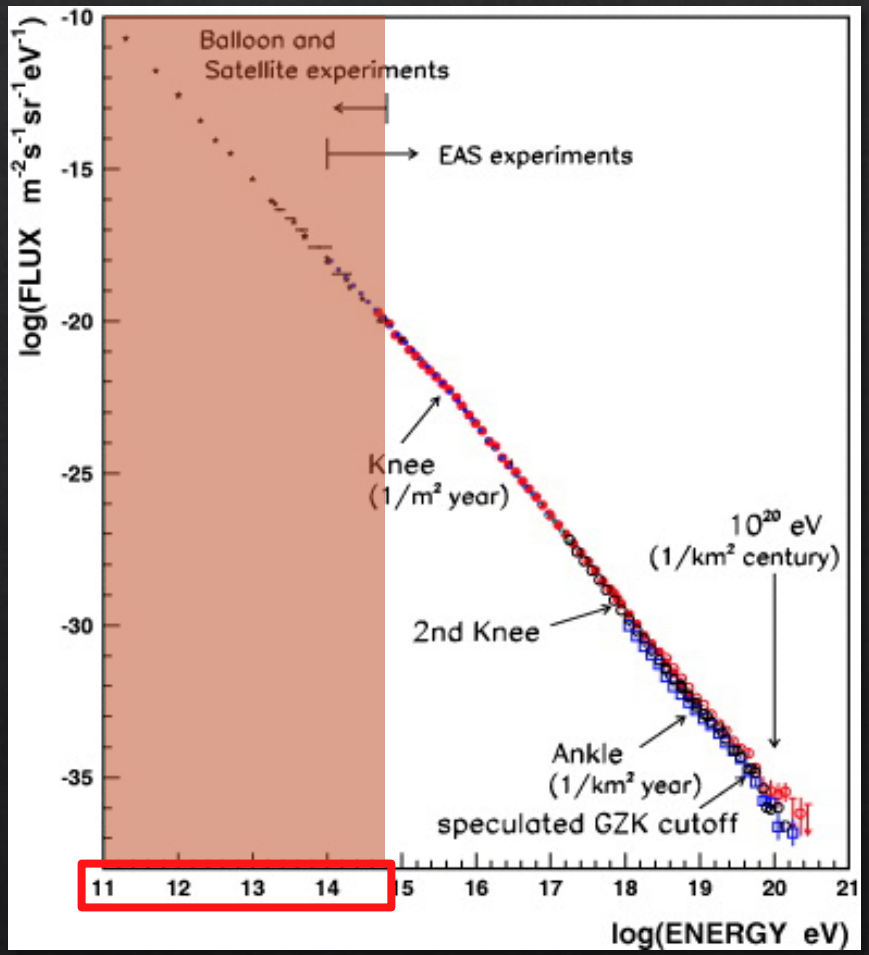

1. Sources and propagation of GCRs in the Galaxy
2. Energy spectrum of GCRs
3. Antimatter in CRs and indirect search for DM

Anisotropy

PROPAGATION OF GCRs (*STANDARD* PICTURE)

Spectrum = **Sources** + **Diffusion** + **Energy losses** + **Convection** + **Fragmentation/ Decay**

$e^{\pm}$

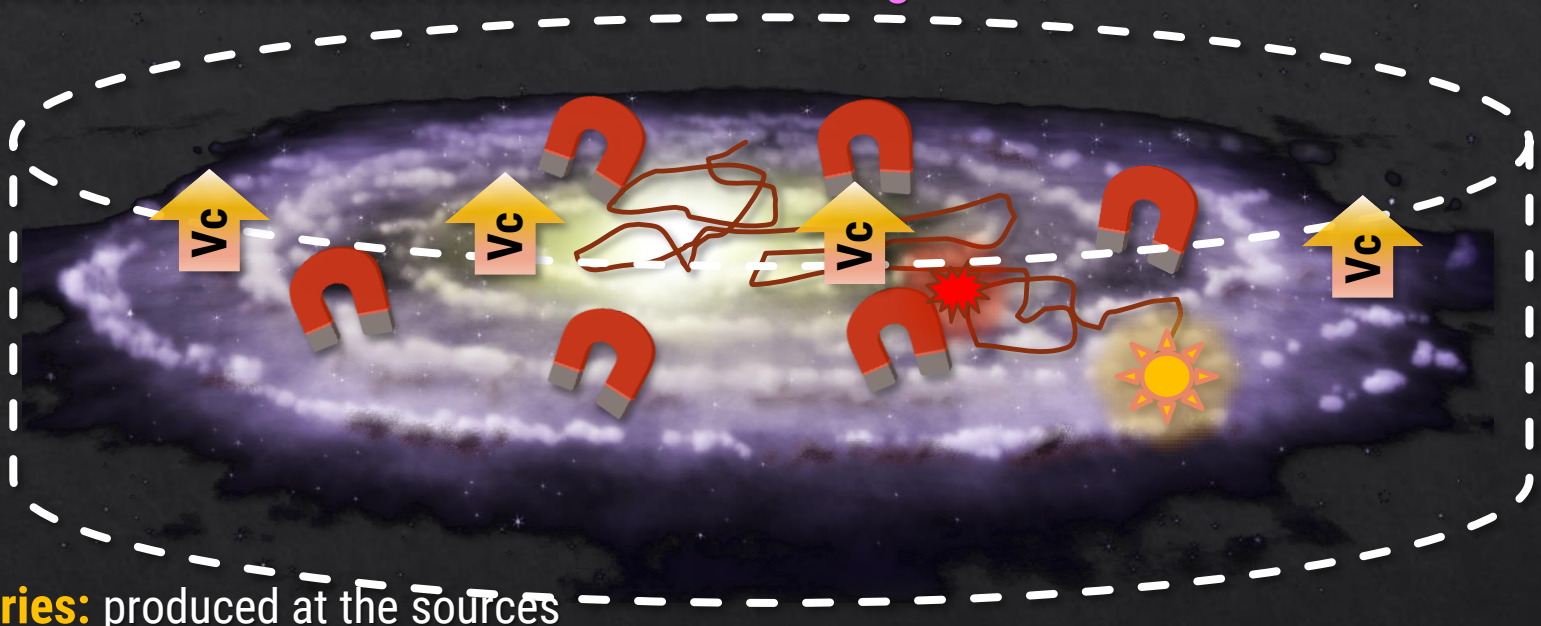

Primaries: produced at the sources

Secondaries: produced in inelastic collisions in the ISM (in particular, antimatter)

The spectrum of GCRs up to few TeV is, essentially, a power law shaped by:

- **Acceleration** at the sources (shock waves)
- **Diffusion** in the random turbulent inhomogeneities of the GMF

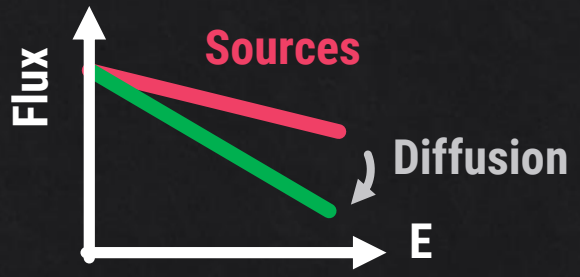

Space-Based Detectors

CALET

(CALorimetric Electron Telescope)

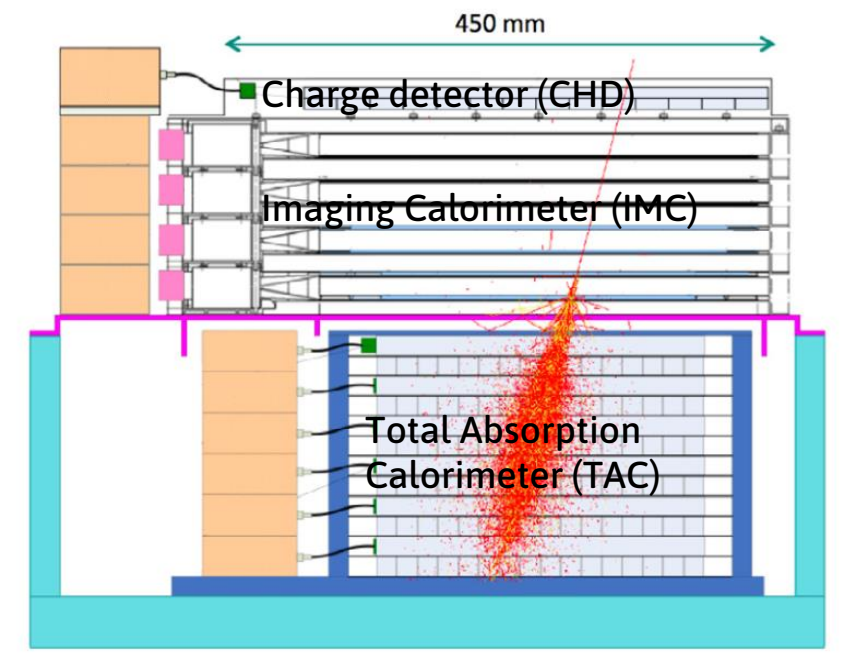

- Data taking: from 2015
- Geom. Factor: ~0,1 m^2sr
- Calorimeter (30 X_0)
- Energy range: up to few tens of TeV

DAMPE

(DArk Matter Particle Explorer)

See M. Stolpovskiy's talk

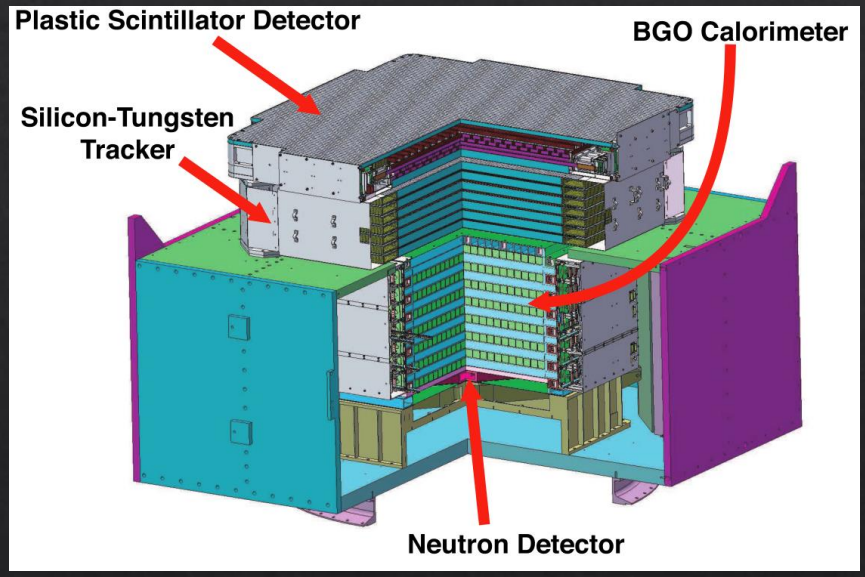

- Data taking: from 2015
- Geom. Factor: ~0.3 m^2sr (e-)
- Calorimeter (32 X_0)
- Energy range: up to 10 TeV (e-)
  up to 100 TeV (nuclei)

Space-Based Detectors

AMS-02

(Alpha Magnetic Spectrometer)

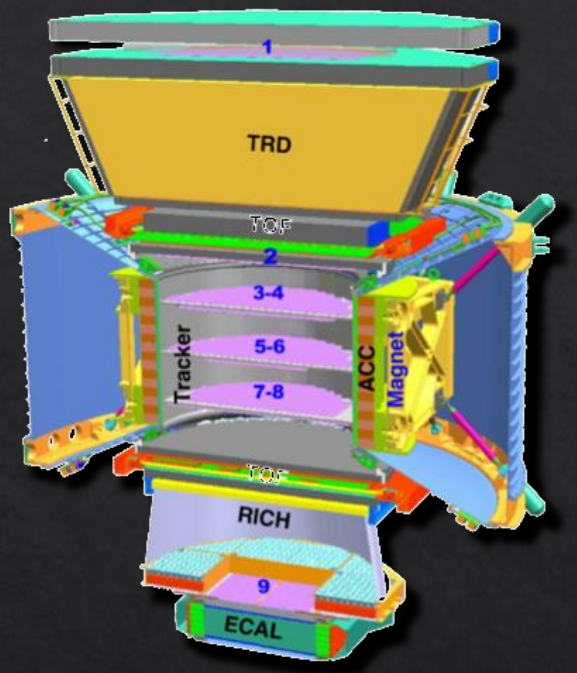

- Data taking: from 2011
- Geom. Factor: ~0.5 m^2sr (Inner)
  ~0.04 m^2sr (ECAL)
- Magnetic spectrometer + Electr. Calorimeter ($17X_0$)
- Energy range: up to few TeV

Fermi-LAT

(Large Area Telescope)

BONUS

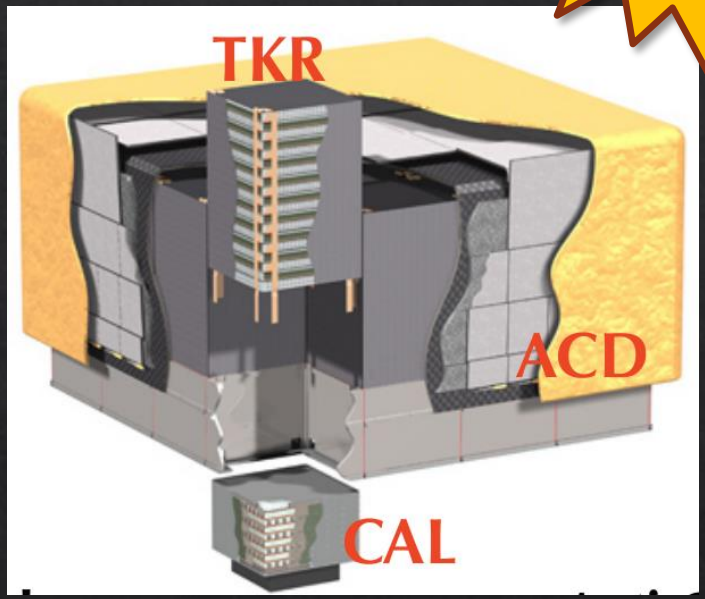

- Pair conversion telescope
- Data taking: from 2008
- Geom. acceptance: ~0.95 m^2sr
- Calorimeter ($8.6\ X_0$)
- Energy range: up to few TeV

Proton Flux

Proton spectrum measured by **AMS-02** shows a **deviation from a single power law** above few hundred GV

AMS-02: [Q. Yan @ ICRC2019]

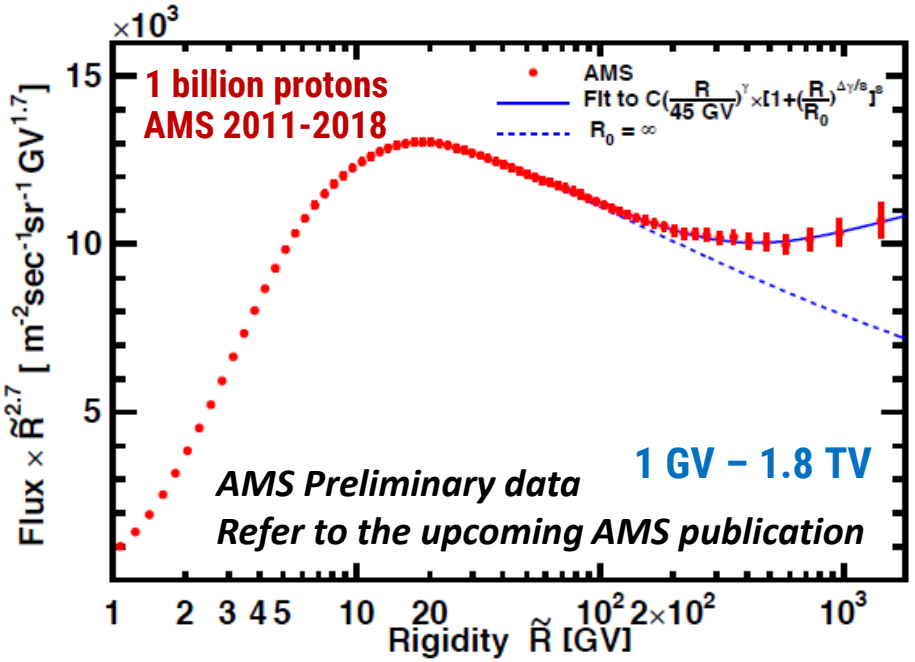

Fermi-LAT: [PoS(ICRC2017) 159]

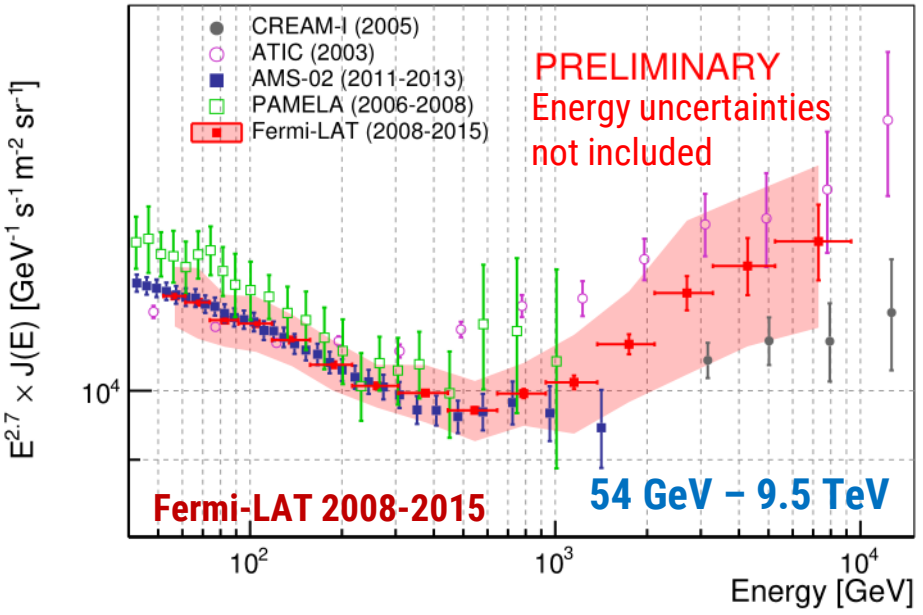

Fermi-LAT proton flux represents the first time a space-based measurement of the cosmic-ray proton spectrum has been able to extend to nearly 10 TeV

Proton Flux

CALET observations are consistent with AMS-02 and confirm the **spectral hardening** with a deviation from a single power law

CALET: [Phys. Rev. Lett. **122**, 181102 (2019)] **DAMPE:** [Sci. Adv. 5 (9) (2019)]

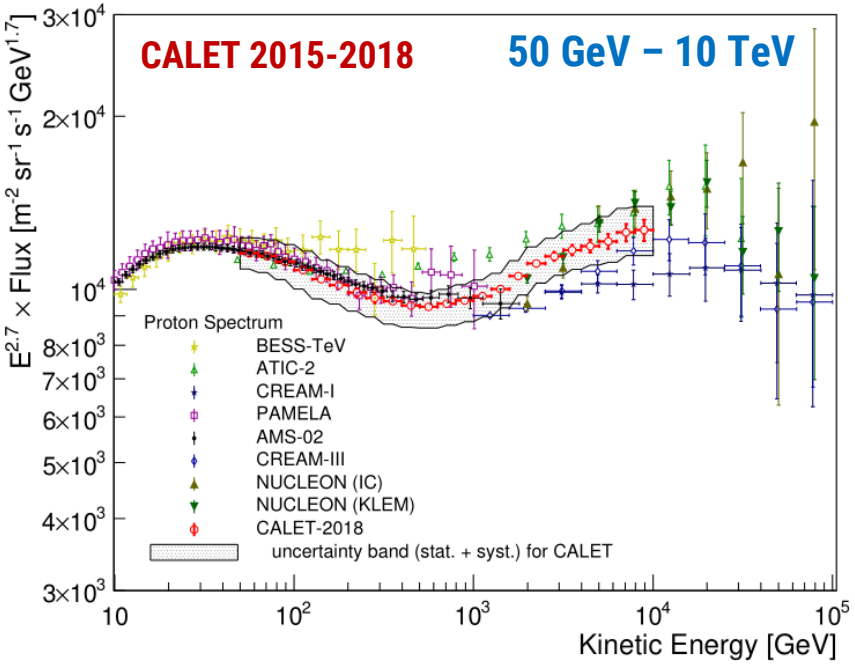

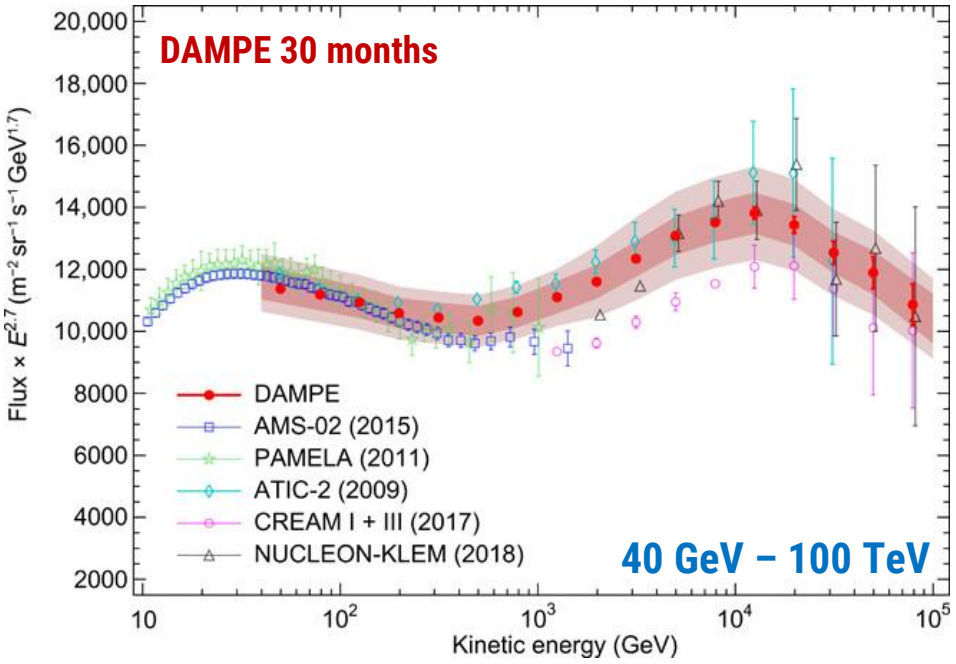

DAMPE measured proton spectrum confirms the **spectral hardening at ~300 GeV** found by previous experiments and reveals a **softening at ~13.6 TeV**

Nuclei Fluxes

AMS-02: [Phys. Rev. Lett. **120**, 021101 (2018)]

Rigidity dependence of Primary and Secondary Cosmic Rays

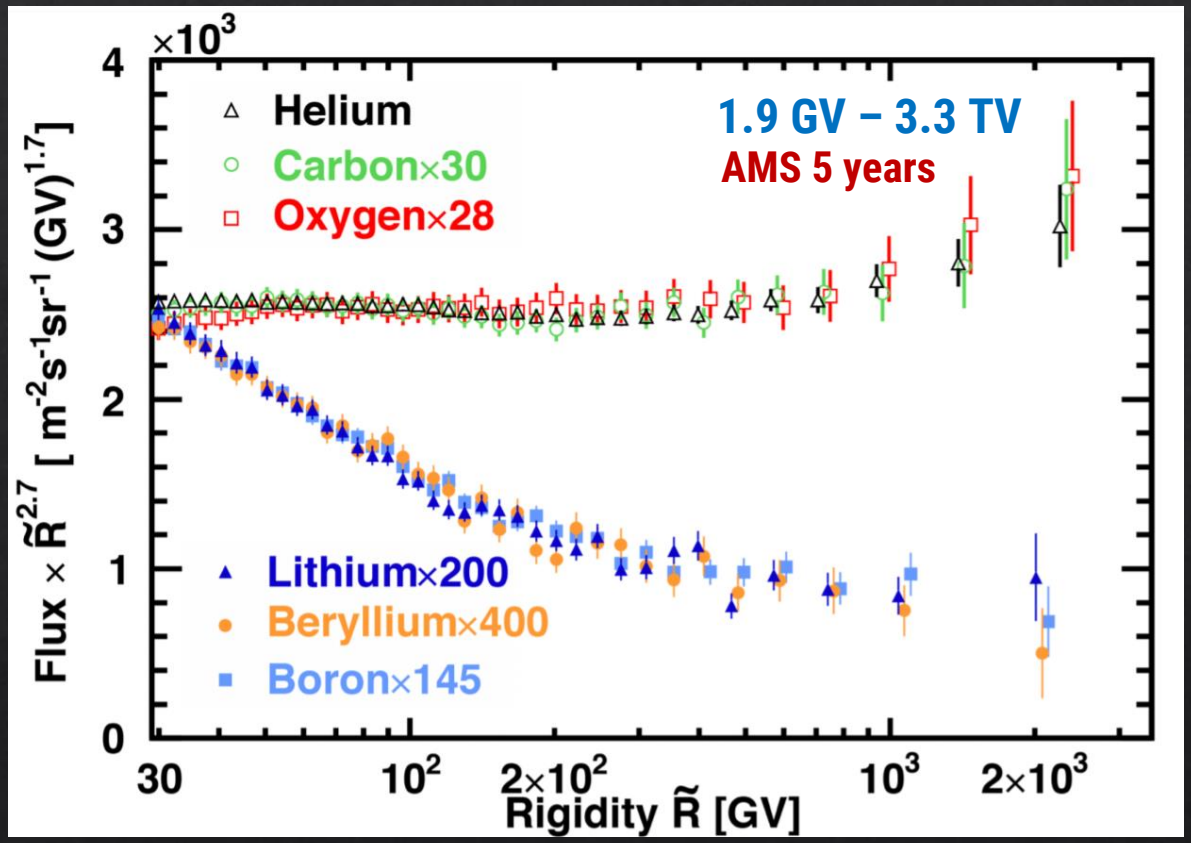

- Rigidity dependences are distinctly different for primaries and secondaries
- Both **deviate from a single power law** above 200 GeV

Nuclei Fluxes

Preliminary results on nuclei fluxes

CALET: [PoS(ICRC2019) 101]
CALET: [PoS(ICRC2019) 034]

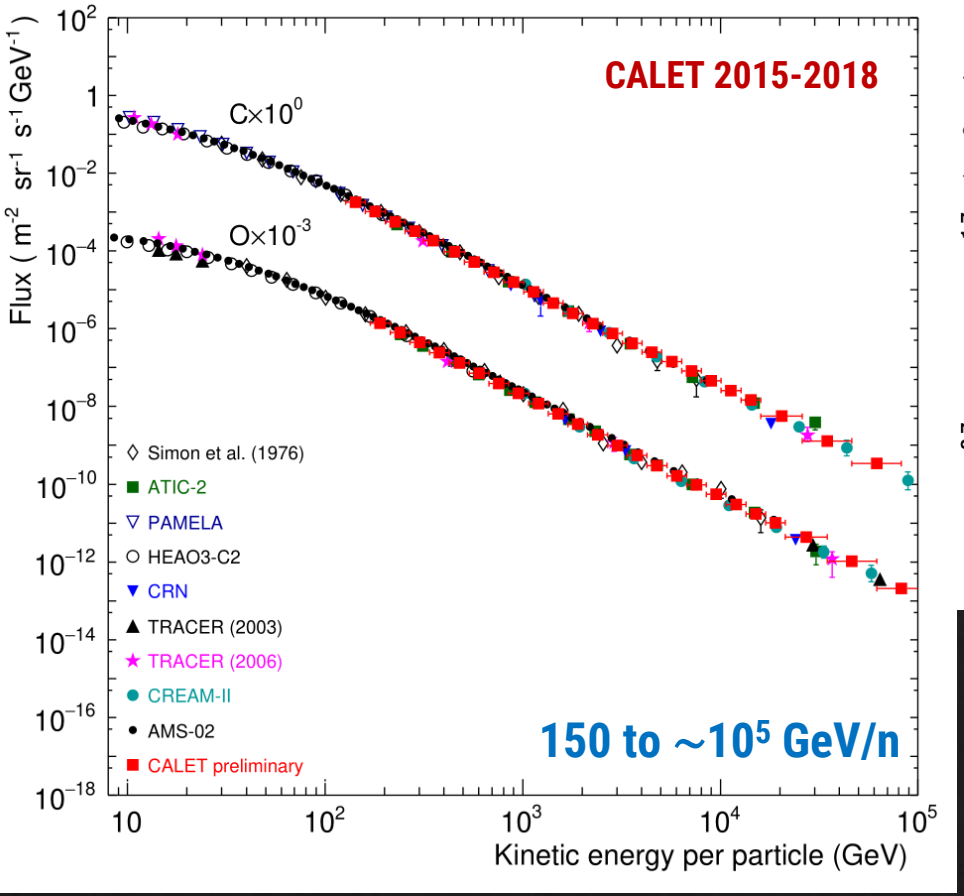

DAMPE: [PoS(ICRC2019) 058)]

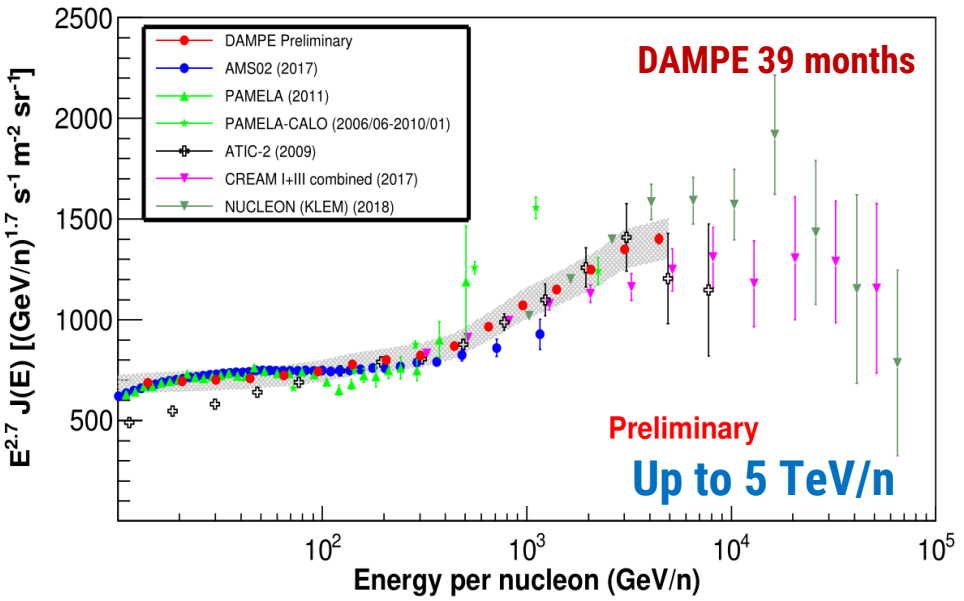

Estimation of the systematic uncertainties ongoing in both cases

Electron & Positron Fluxes

AMS Positron spectrum
[Phys. Rev. Lett. **122**, 041102 (2019)]

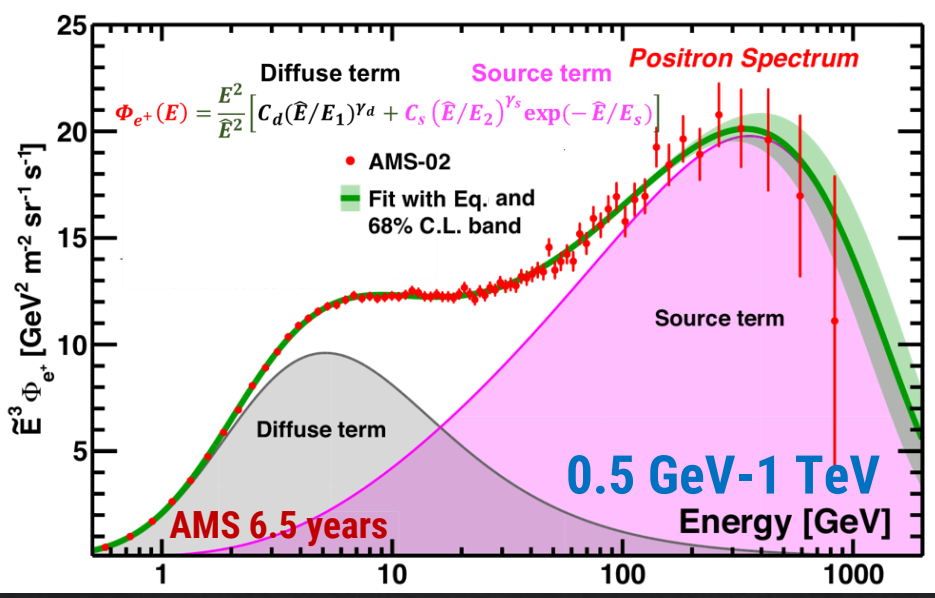

AMS Electron spectrum
[Phys. Rev. Lett. **122**, 101101 (2019)]

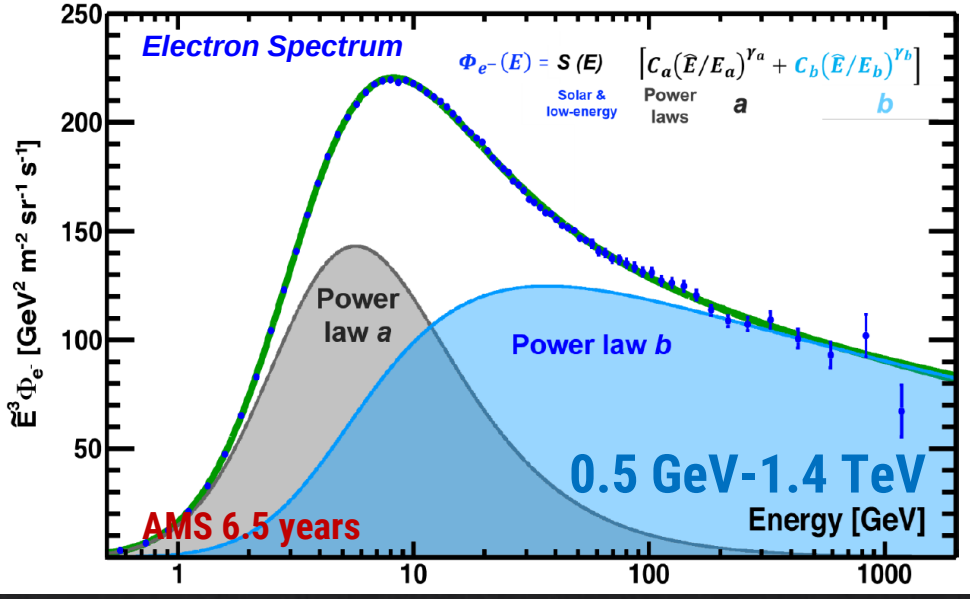

- Significant **excess above 25 GeV**, a sharp dropoff above 284 GeV, and a finite exponential energy cutoff at 810 GeV
- **Non consistent with a pure secondary origin** of positrons
- The observation may require the inclusion of **primary sources of positrons**

- Significant **excess above 42 GeV** non consistent with lower energy trends
- Well described by the **sum of two power law contributions** in the entire range

All-Electron Spectrum

DAMPE: [G. Ambrosi *et al*., Nature **552**, 63–66 (2017)]
CALET: [O. Adriani *et al.* Phys. Rev. Lett. **120**, 261102 (2018)]

DAMPE: Direct detection of a **spectral break** at E ≈ 0.9 TeV, with the spectral index changing from $\gamma_1 \approx 3.1$ to $\gamma_2 \approx 3.9$

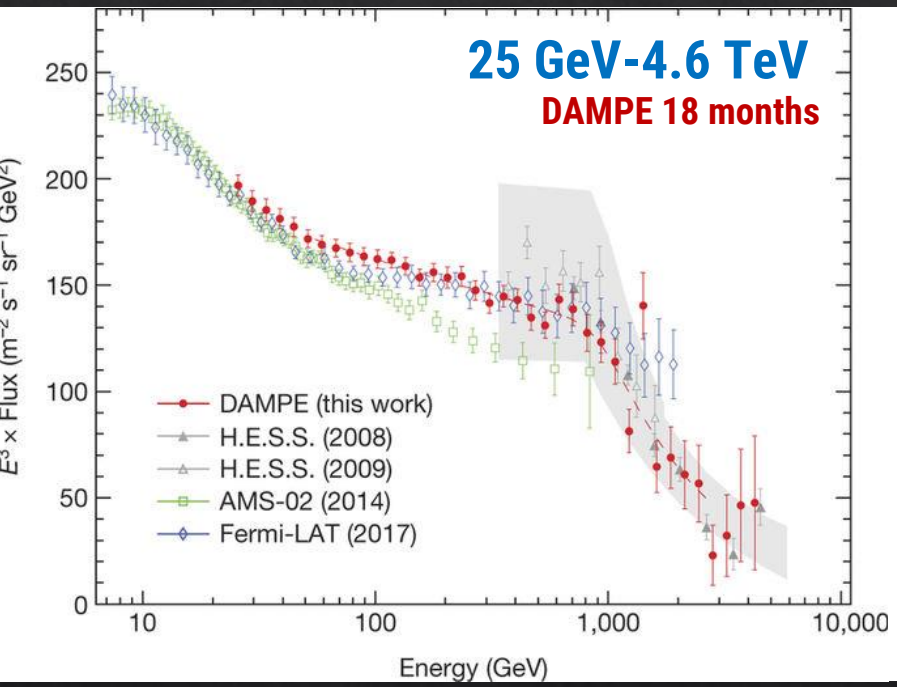

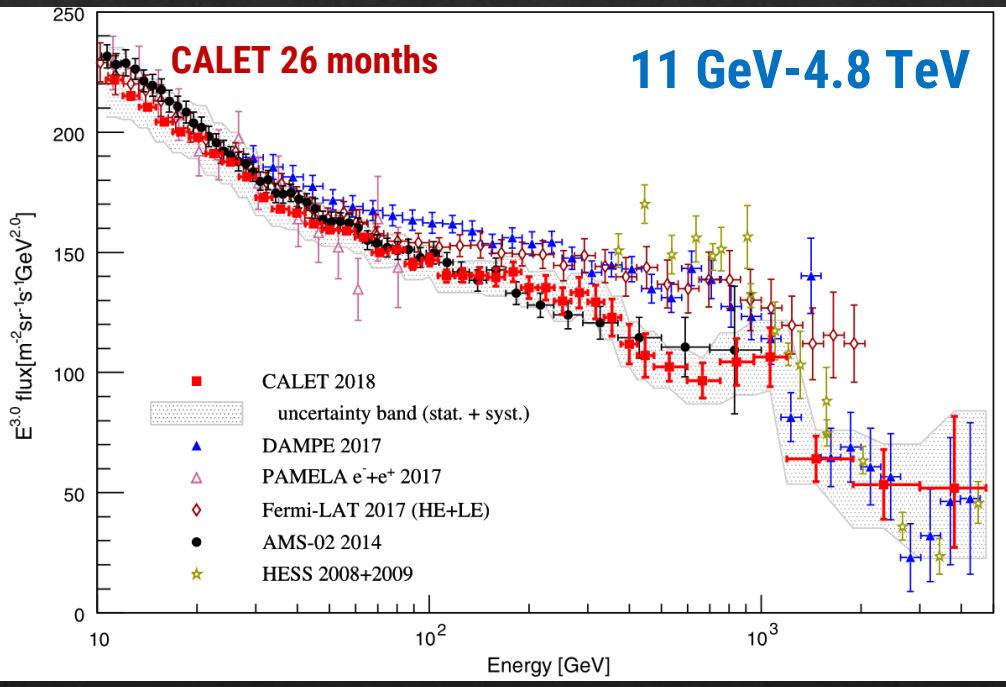

CALET: The TeV region shows a **suppression of the flux** compatible with the DAMPE results. The determination of the break will improve with better statistics

Possible Interpretations

Spectral hardening above few hundred GV in proton and nuclei spectra

- Local sources of high rigidity proton & nuclei CRs [G. Bernard *et al.*, A&A 555, A48 (2013)]
- Different acceleration mechanisms at the source [V. Ptuskin *et al.*, ApJ 763(1):47, (2013)]
- Modification of CR transport models [R. Aloisio *et al.*, A&A 583, A95 (2015)]

Electron and positron spectral features

- Local sources of high energy electrons and positrons [M. Di Mauro *et al.*, JCAP04(2014)006]
- High energy positrons produced via DM annihilation [L.A. Cavasonza *et al.*, ApJ 839 (2017)]
- Modified CR propagation models [K. Blum *et al.*, PRL 111:211101 (2013)]

The measurement of the **anisotropy** provides complementary information to the features observed in the spectra and may help understand their origin

Anisotropy with Space-Based Detectors

Traditionally, the search for anisotropies in CRs has been carried out by **ground-based detectors**

CR anisotropy measurements with **space-based detectors** represent a good opportunity to address the open questions in GCRs in the **precision era**

Ground-based detectors:

- Fix position in the Earth ⇒ partial sky coverage
- Detector efficiencies hard to evaluate
- Usually, insensitive to declination ⇒ projection of the dipole onto the equatorial plane

Space-based detectors:

- Nearly full coverage of the skymap
- 3D characterization of the dipole anisotropy
- Direct identification of the primary CR species
- Precision determination of detector efficiencies

AMS-02: Sky Coverage

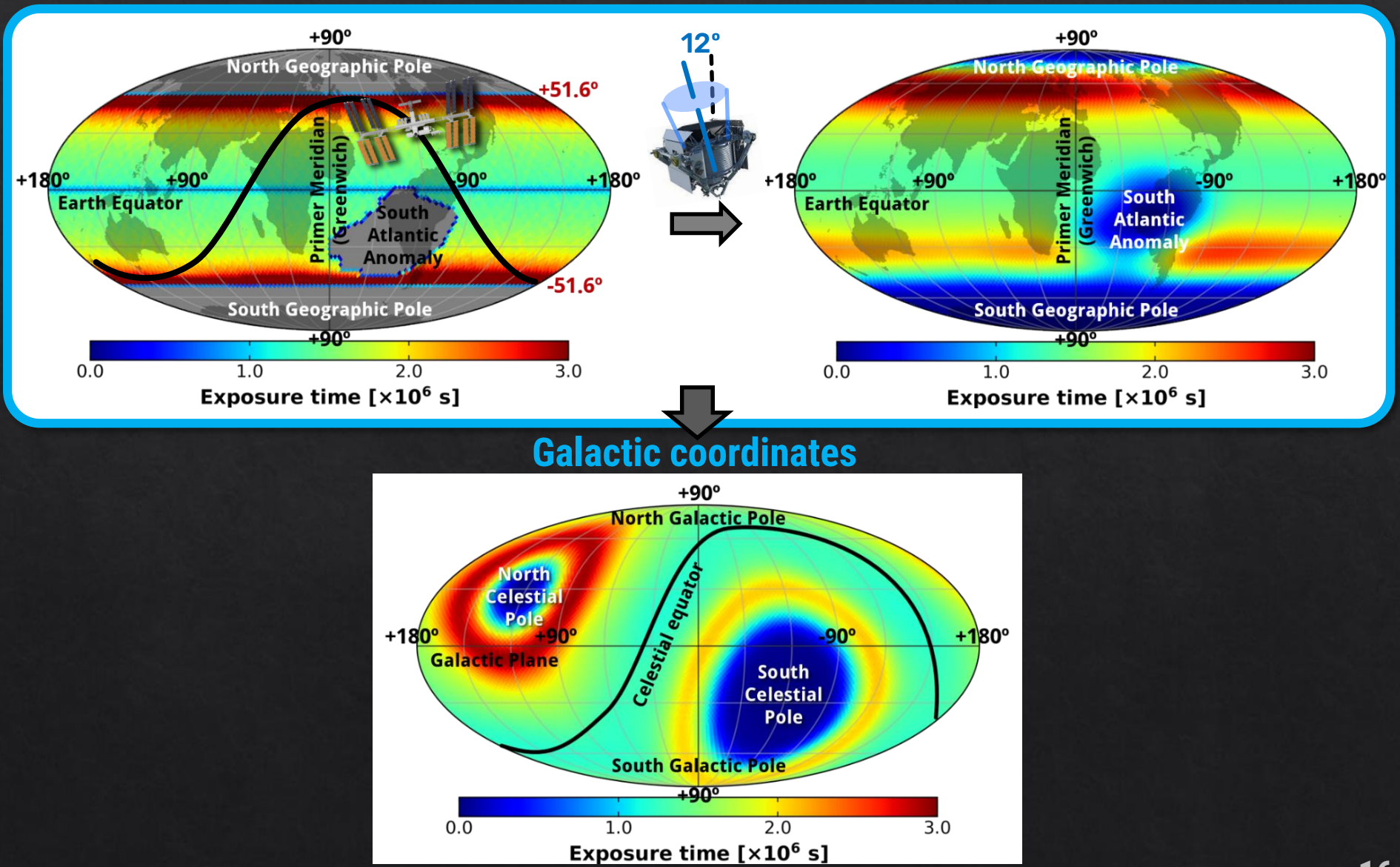

AMS-02: Positron Anisotropy

Sample selection

Proton background is reduced below the percent level with a selection based on cuts on E/p and the TRD and ECAL estimators

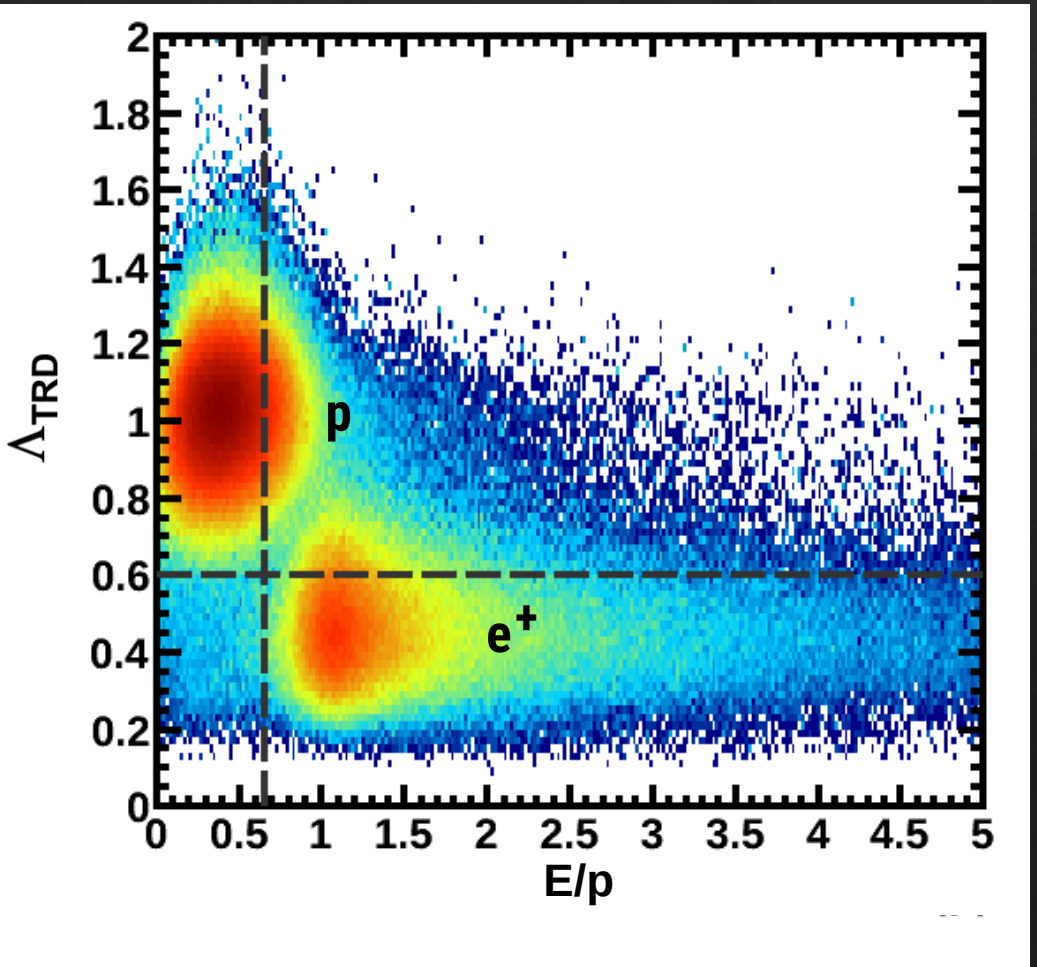

Events are selected well above the maximum geomagnetic cutoff within acceptance at the different locations in the ISS orbit

For the anisotropy analysis, selected events are grouped into **5 cumulative energy ranges**:

***E* > 16**, **25**, **40**, **65**, and **100 GeV**

Event Sample: AMS 6.5 years

9.9×10^4 e^+ ($16 < E < 350$ GeV)

AMS-02: Positron Anisotropy

The arrival directions of **positron events** are compared to the expected map for an **isotropic** flux in **Galactic coordinates**

$16 < E < 350$ GeV

9.9×10^4 positrons | **Isotropic map**

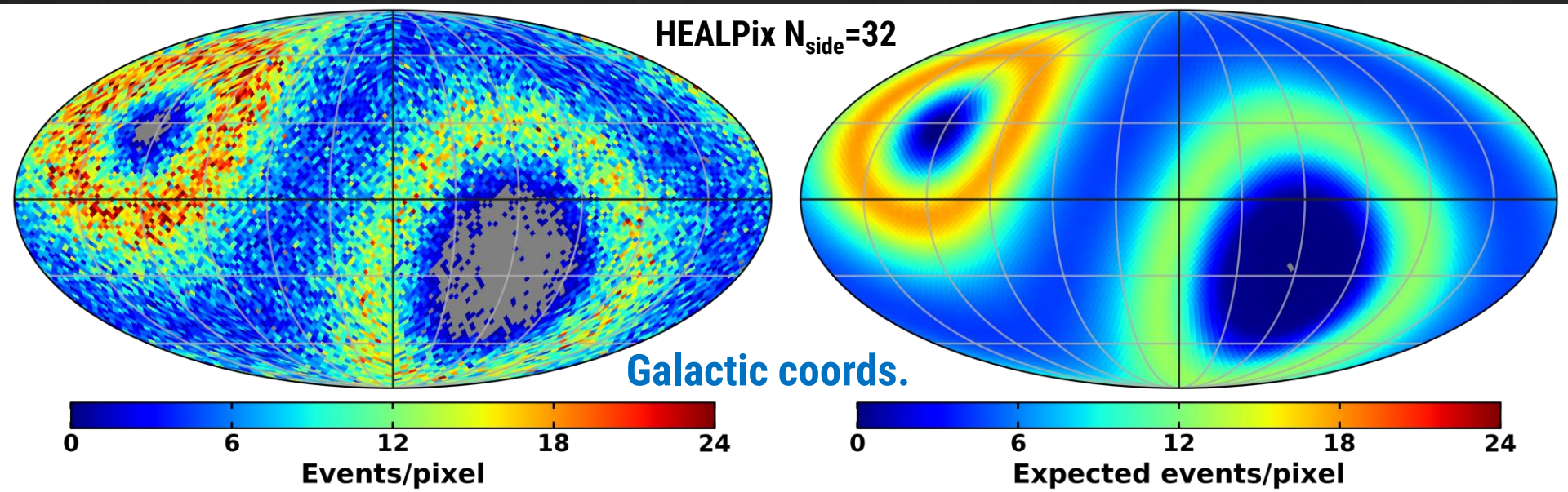

AMS-02: Positron Anisotropy

Computation of **isotropic map** requires detailed understanding of **detector efficiencies** at different **geographical locations**

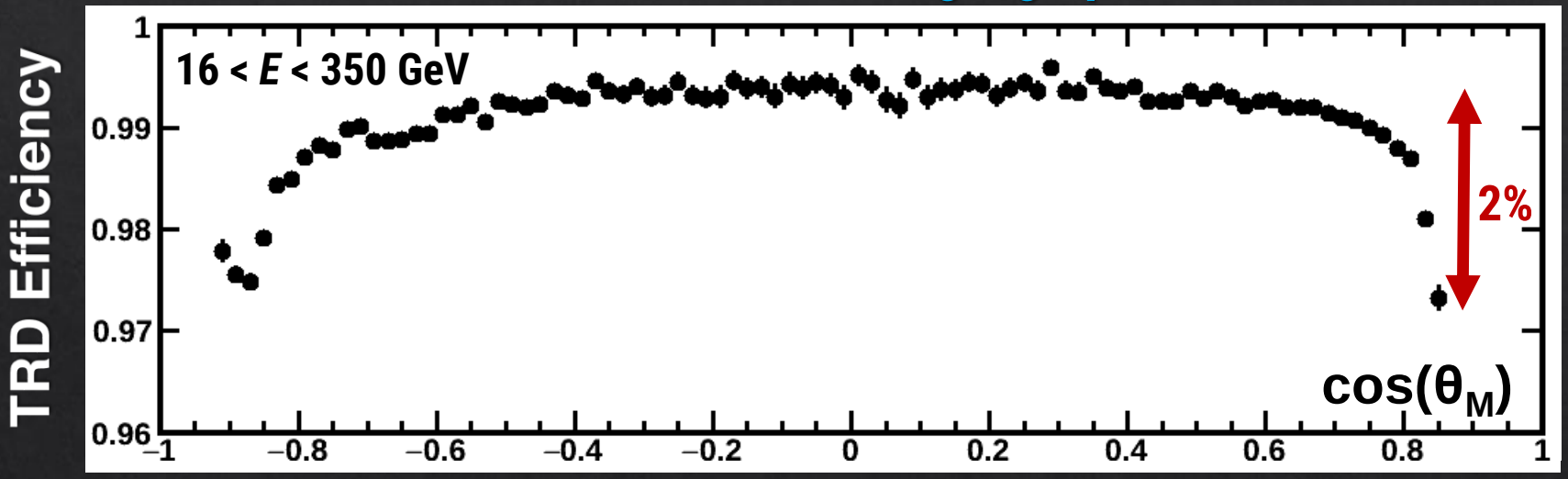

Geographical Coordinates (ISS Position)

16 < *E* < 350 GeV

Galactic Coordinates

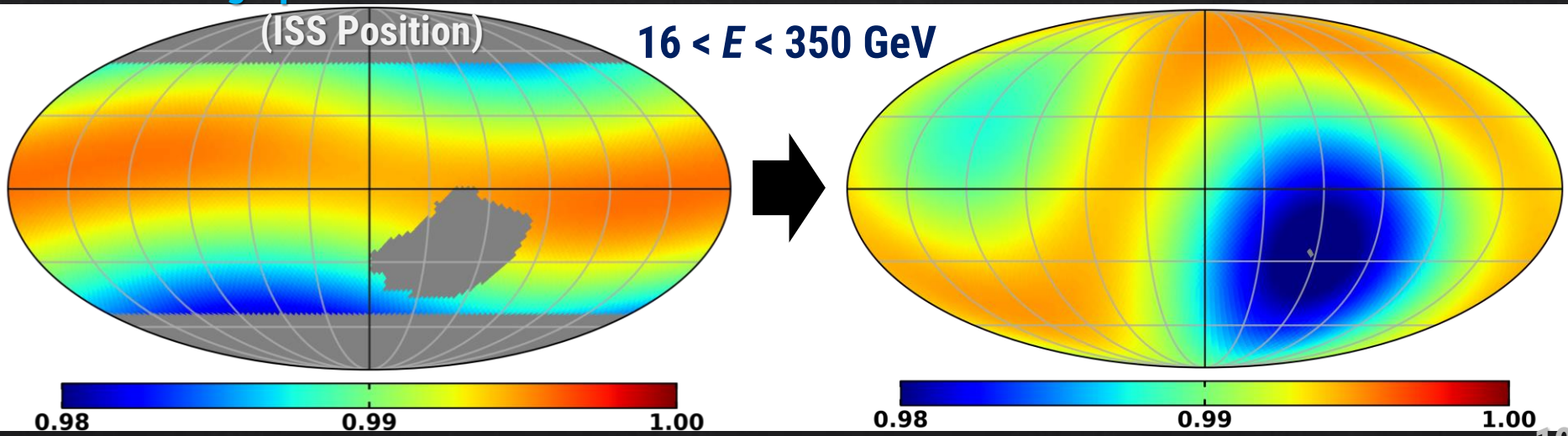

AMS-02: Positron Anisotropy

Sky map of the **relative fluctuation** of the positron arrival directions in **galactic coordinates**

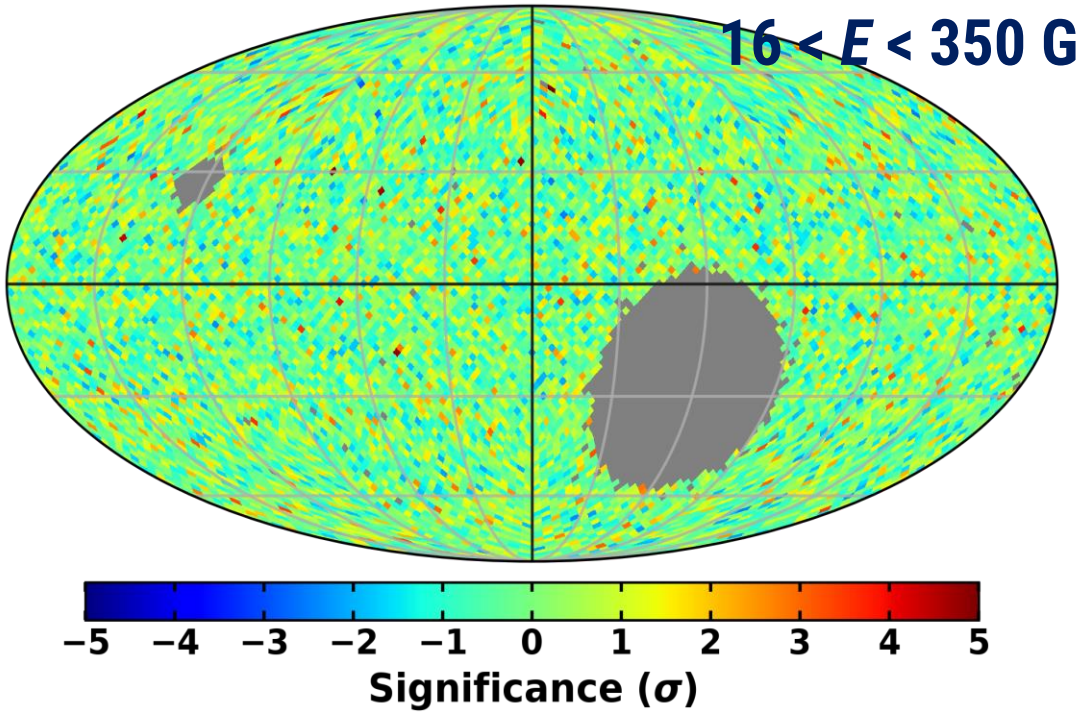

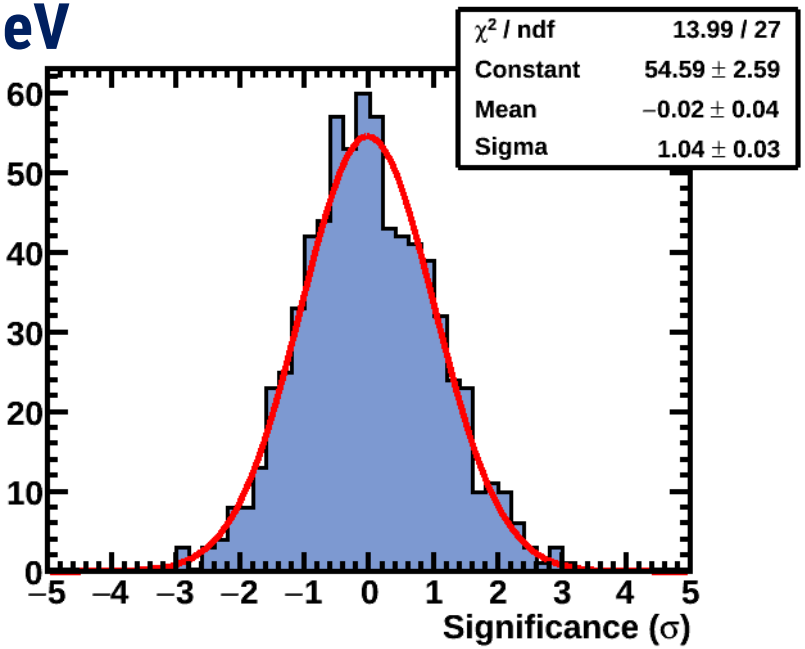

The observed sky map shows **no evident pattern or structures**

A **likelihood fit** is used to compare the distribution of events and the reference map, and takes into account the differences in the exposure for different energies due to geomagnetic cutoff

AMS-02: Positron Anisotropy

Results consistent with **isotropy**

Upper limits are set for each energy range

Amplitude of the dipole anisotropy on e^+ for $16 < E < 350$ GeV

$\delta < 1.9\%$ at the 95% C.I.

[Phys. Rev. Lett. **122**, 041102 (2019)]

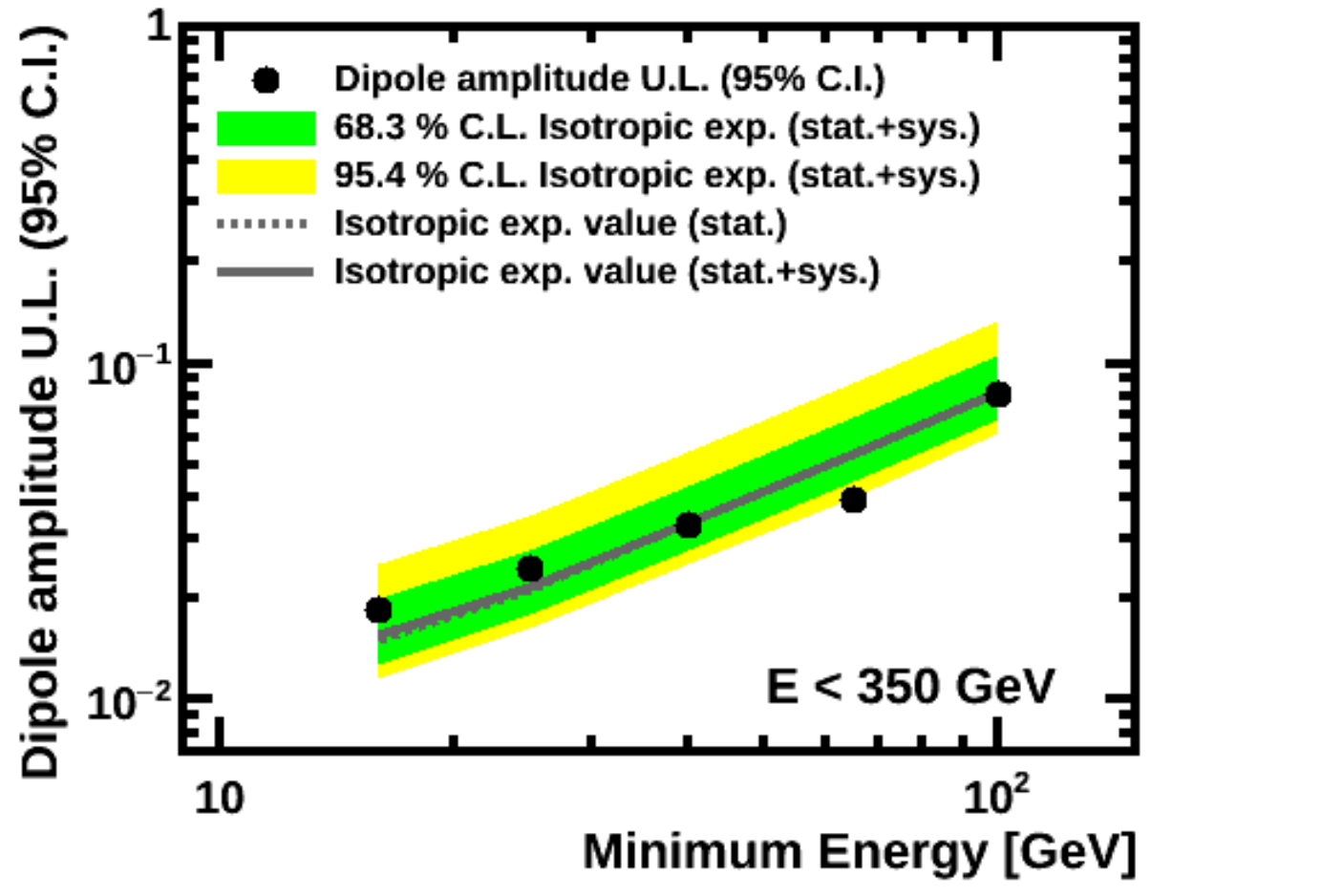

AMS-02: Electron Anisotropy

In addition to the sensitivity to nearby astrophysical sources, the measurement of electron anisotropy provides a test of systematics for the positron analysis

Amplitude of the dipole anisotropy on e^- for $16 < E < 350$ GeV

$\delta < 0.5\%$ at the 95% C.I.

[Phys. Rev. Lett. **122**, 101101 (2019)]

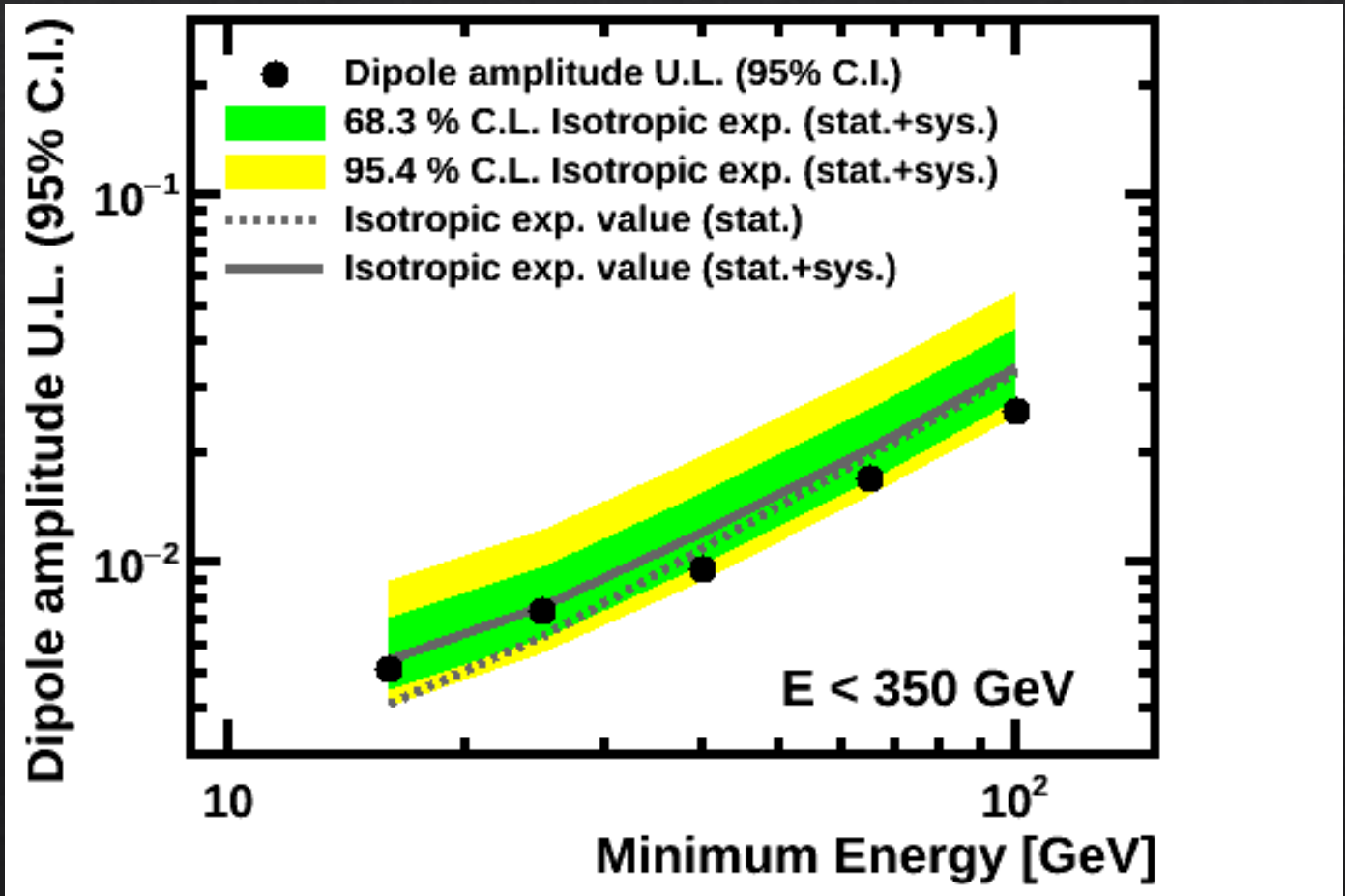

AMS-02: Proton Anisotropy

The arrival directions of **proton events** collected in the first **7.5 years** are compared to the expected map for an **isotropic** flux in **Galactic coordinates**

Selected events are grouped into 9 cumulative rigidity ranges with
R **> 18, 30, 45, 80, 150, 200, 300, 500** and **1000 GV**

1.3×10^8 protons | **Isotropic map**

R **> 18 GV**

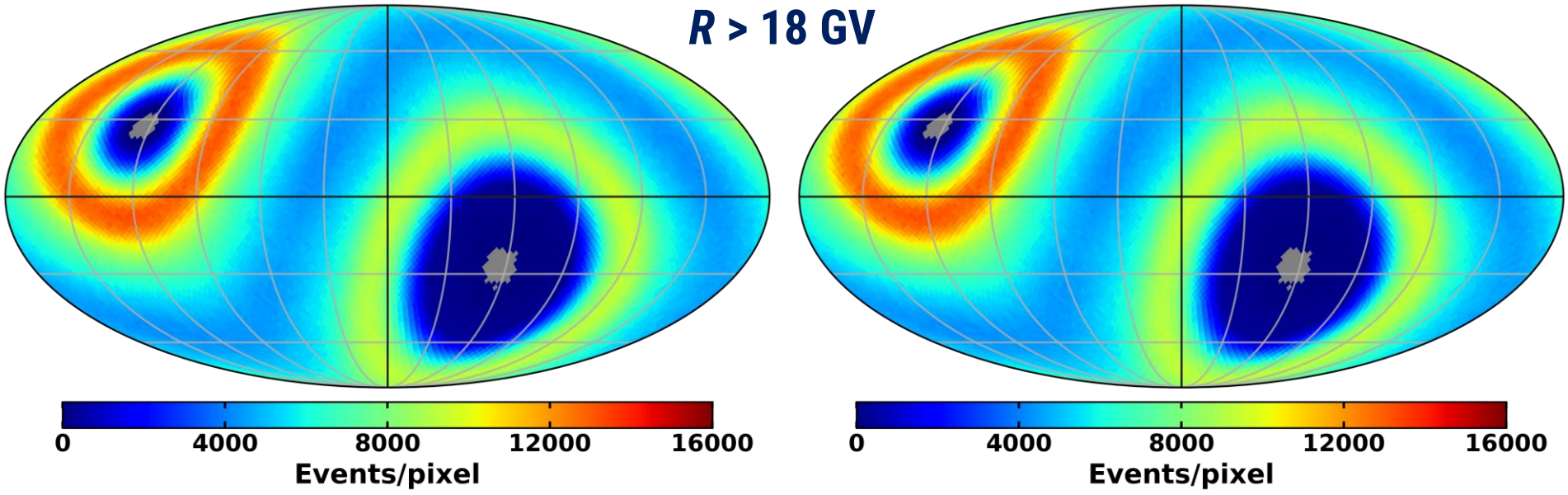

AMS-02: Proton Anisotropy

Computation of **isotropic map** requires detailed understanding of **detector efficiencies** at different **geographical locations**

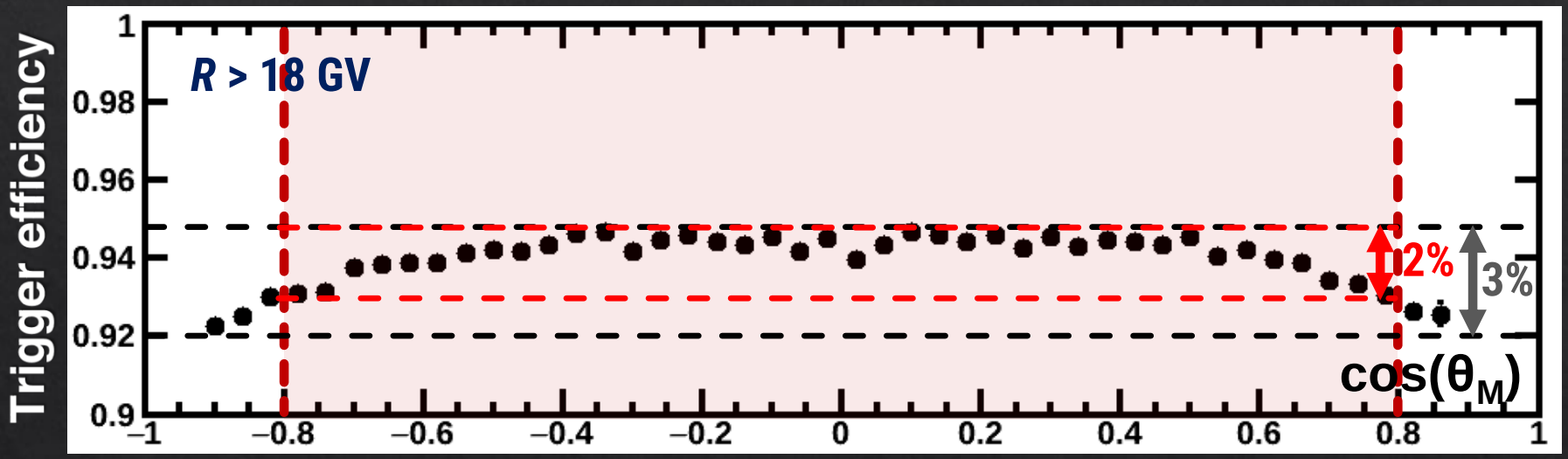

Geographical Coordinates (ISS Position)

R > 18 GV

Galactic Coordinates

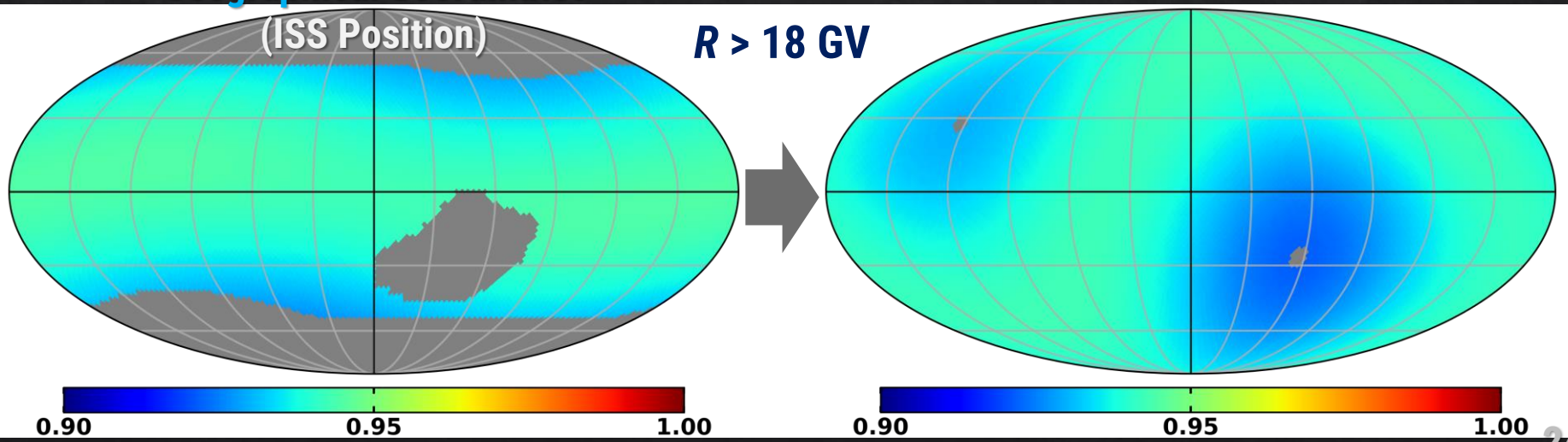

AMS-02: Proton Anisotropy

Results consistent with **isotropy** and **upper limits** are set for each rigidity range

Amplitude of the dipole anisotropy on protons
for $R > 200$ GV (2×10^6 events)
$\delta < 0.38\%$ at the 95% C.I.

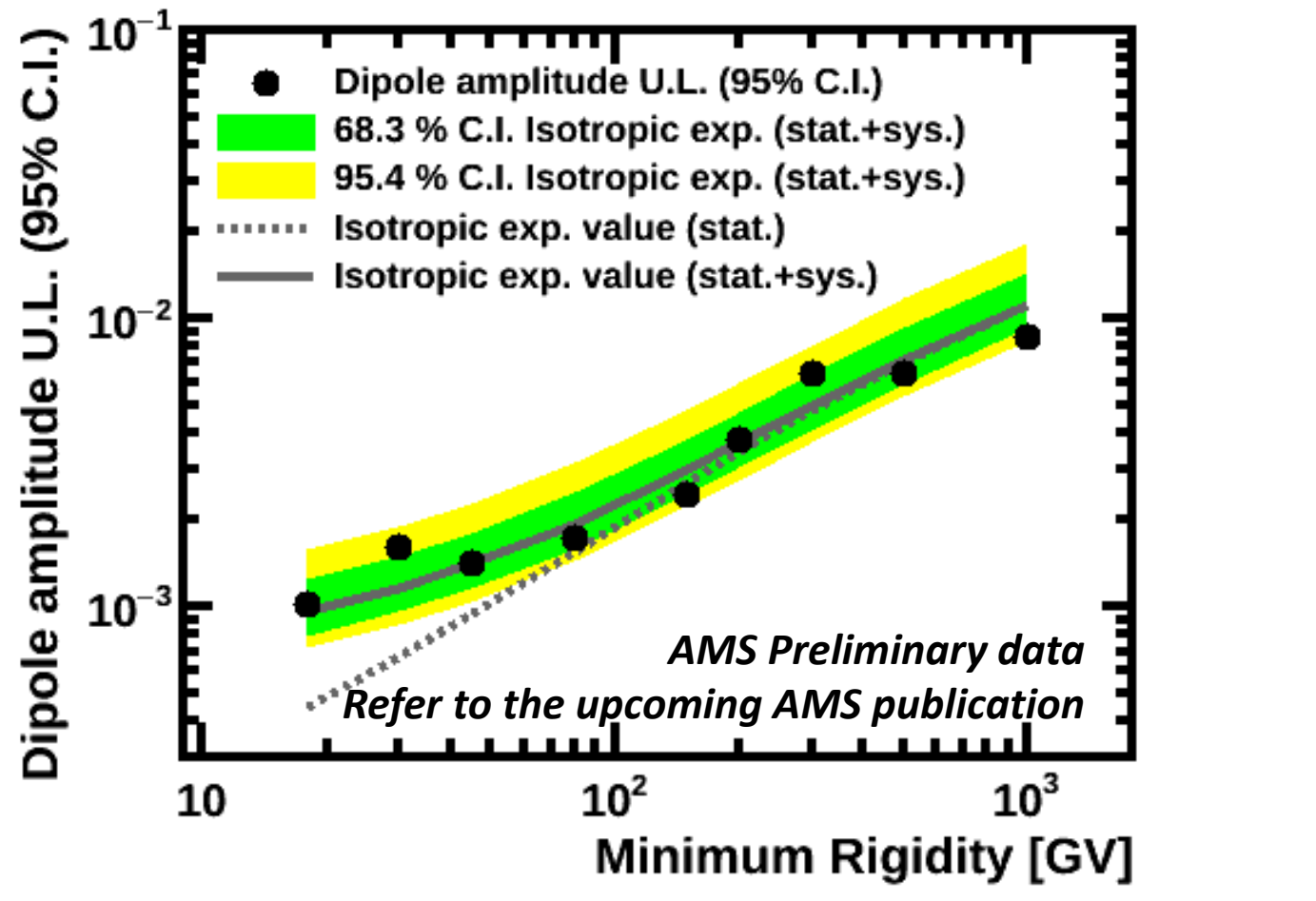

AMS-02: Helium, Carbon & Oxygen Anisotropy

- Similar analysis applied to the **He**, **C** and **O** samples collected in **7.5 years**
- Reduced amplitude of the geographical dependence of the detector efficiencies allows to use **extended detector acceptance**

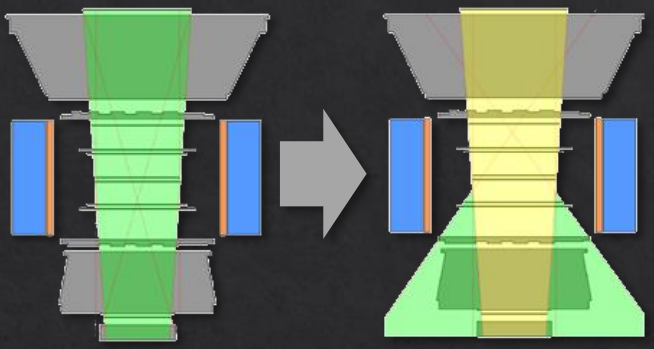

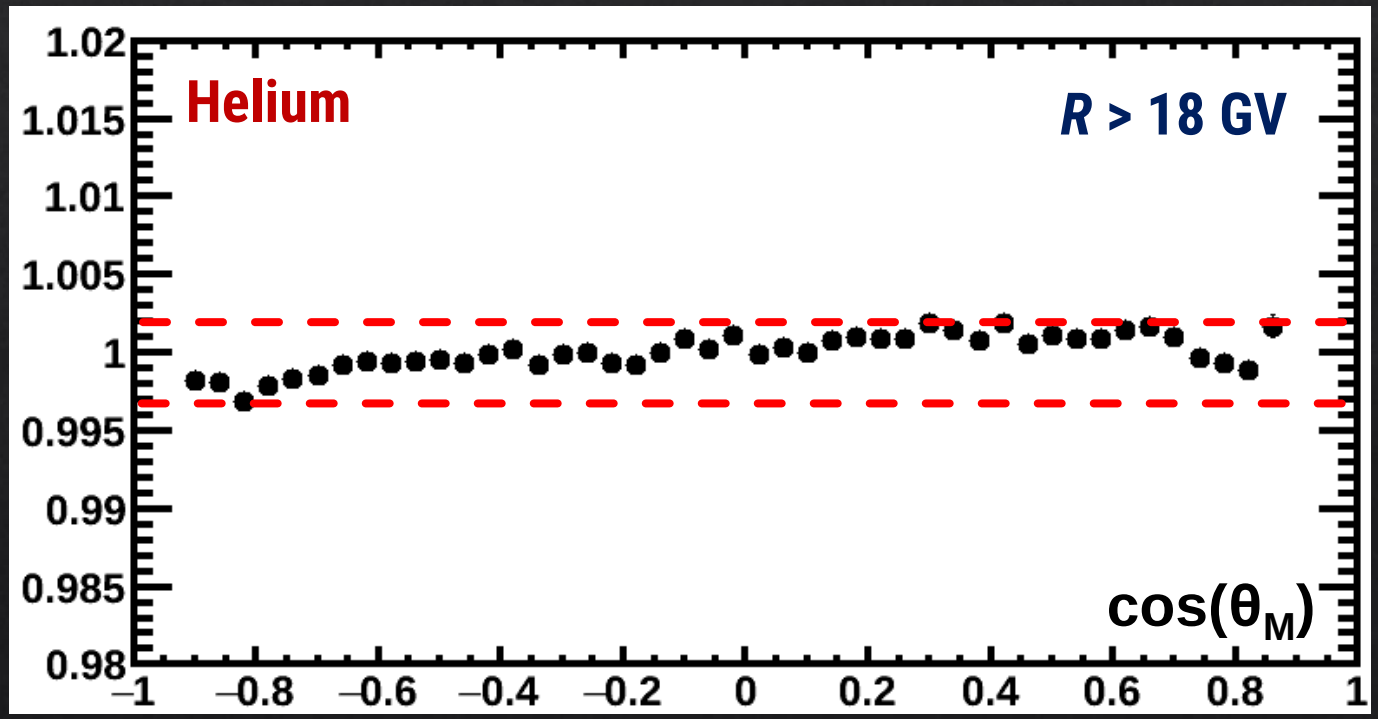

AMS-02: Helium, Carbon & Oxygen Anisotropy

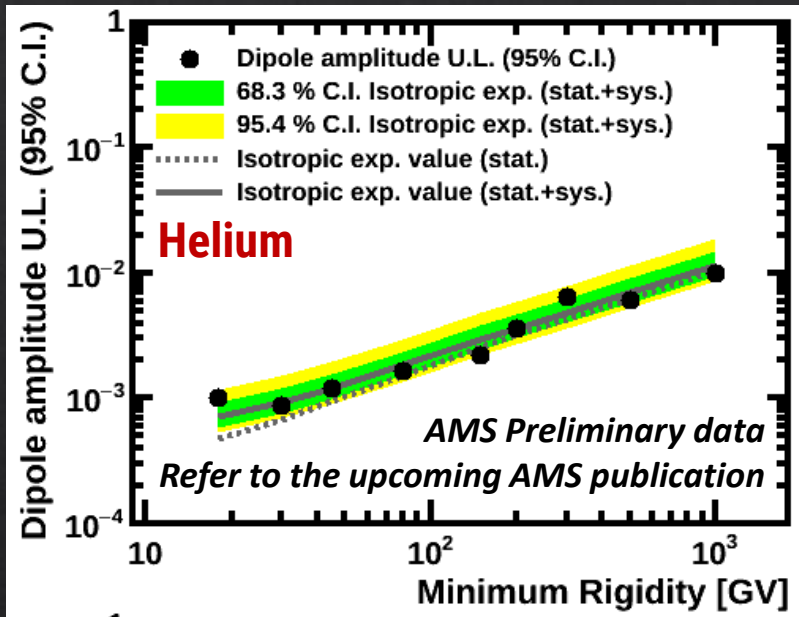

All measurements found compatible with **isotropy** and **upper limits** to the amplitude of the dipole component are set

Helium: **δ < 0.36%** for $R > 200$ GV (2.2×10^6 He)

Carbon: **δ < 1.9%** for $R > 200$ GV (6.1×10^4 C)

Oxygen: **δ < 1.7%** for $R > 200$ GV (6.3×10^4 O)

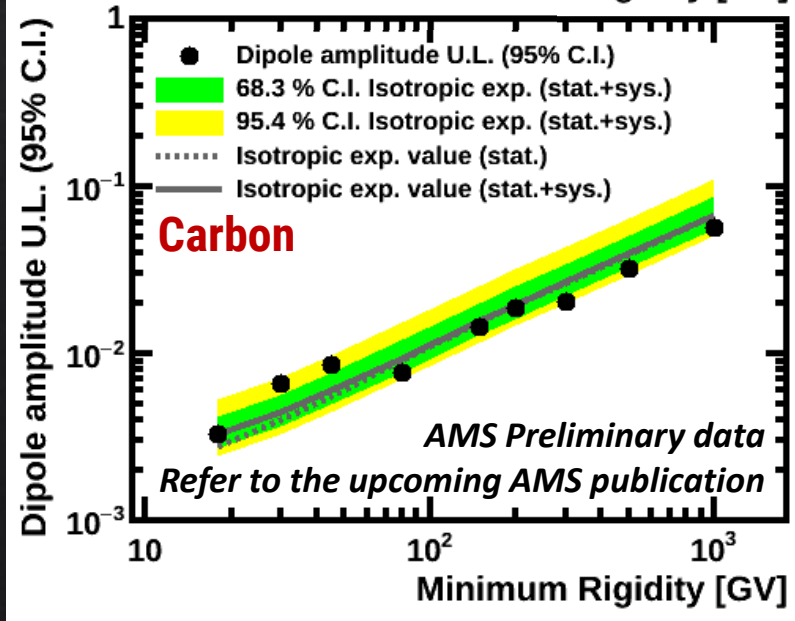

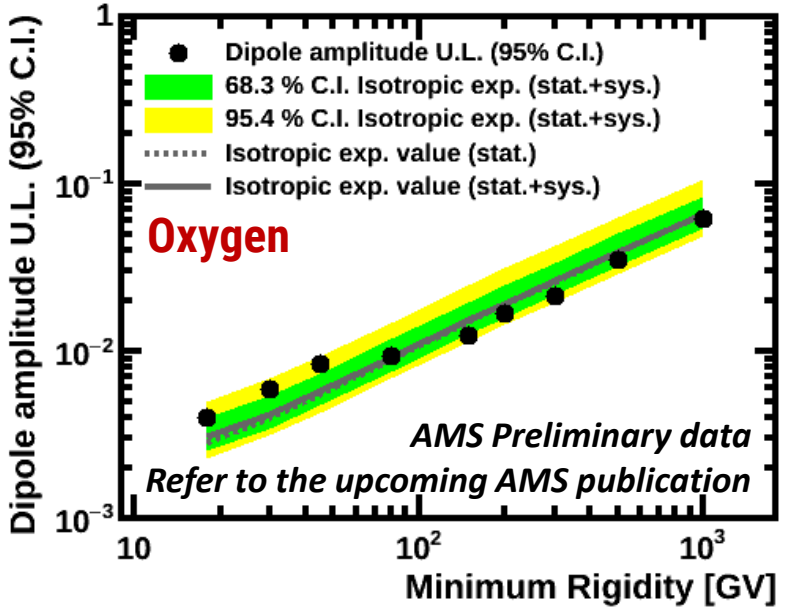

DAMPE Anisotropy

All particle anisotropy

See M. Stolpovskiy's talk

Analysis based on one year of the DAMPE data for all particle types at calorimeter energies from 100 to 500 GeV

Relative intensity map

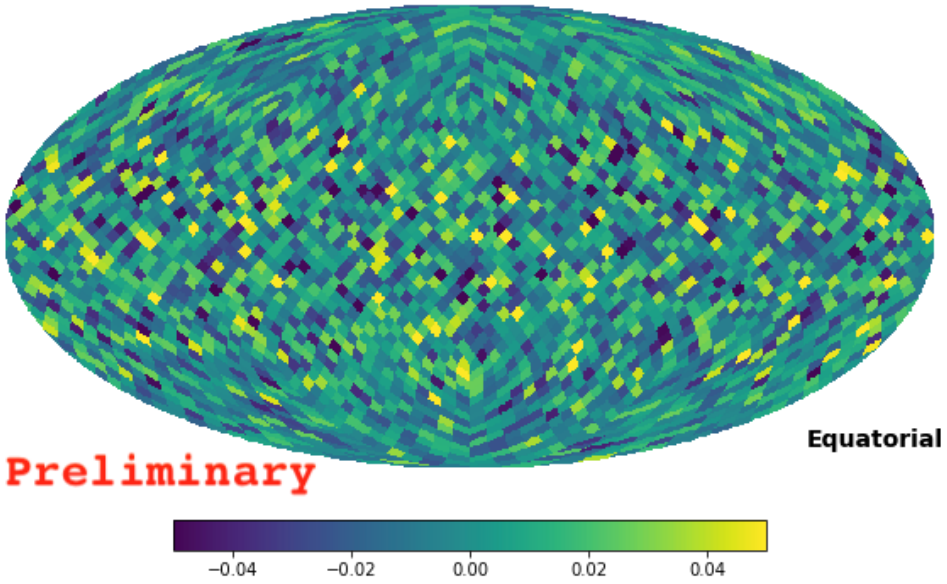

Angular power spectrum

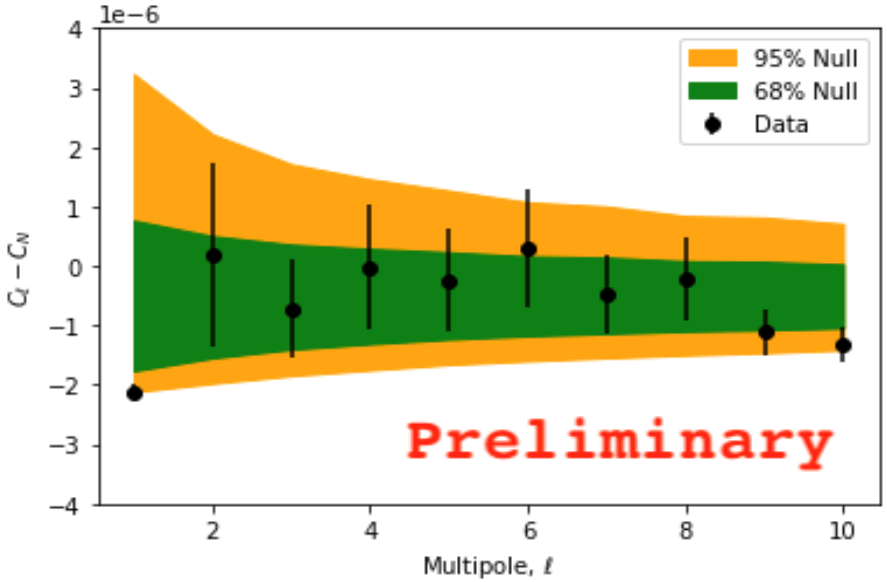

The 95% C.L. upper limit on the dipole amplitude is found to be 4×10^{-3} at this energy range

Fermi-LAT: Proton Anisotropy

[J. Vanderbroucke @ ICRC2019 & arXiv:1903.02905]

Sample selection

- Protons are separated from helium and heavier nuclei by means of cuts on two independent measurements of the charge
- Protons are separated from electrons by means of the Fermi-LAT electron classifier, which exploits the shower shape in the calorimeter

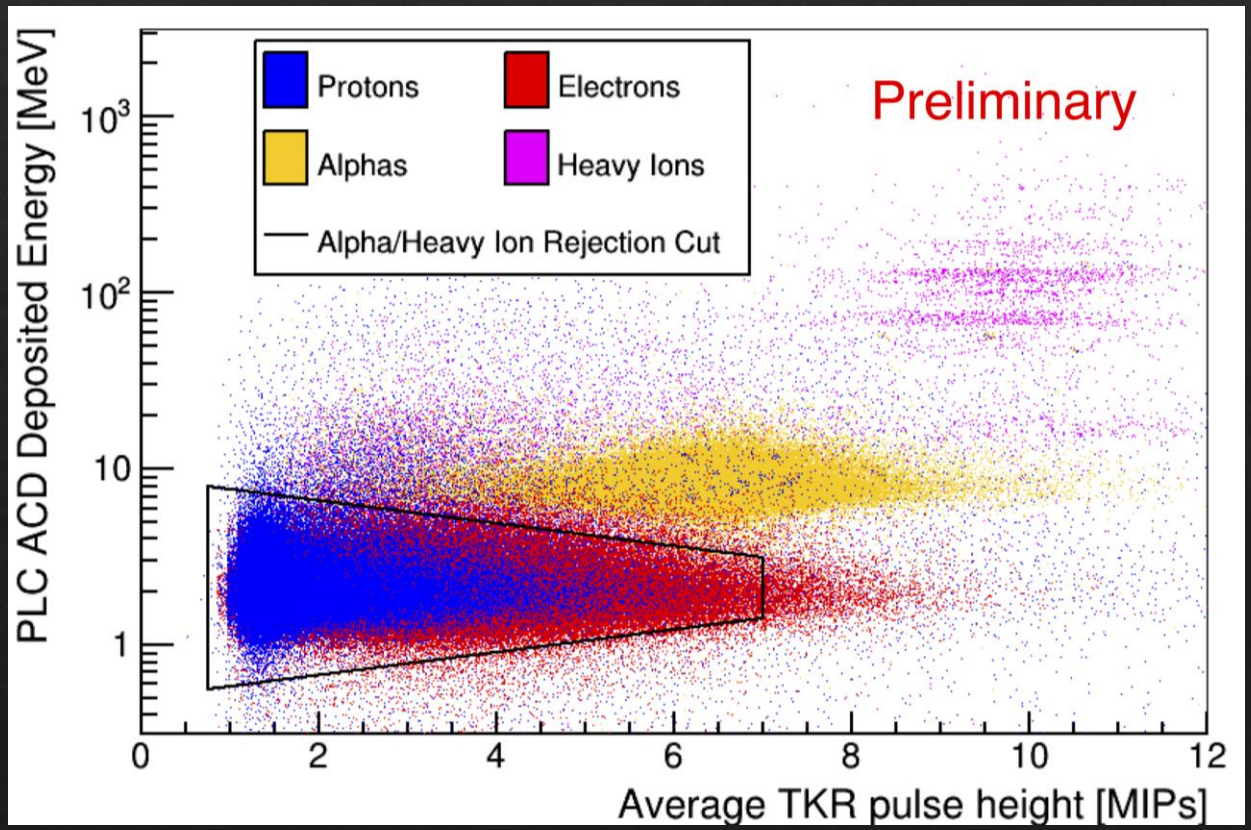

Fermi-LAT: Proton Anisotropy

[J. Vanderbroucke @ ICRC2019 & arXiv:1903.02905]

Analysis based on **8 years of data** (~179 million protons above 78 GeV)
Events are divided into **8 cumulative energy bins** of minimum energy
logarithmically-spaced between ~80 GeV – 10 TeV

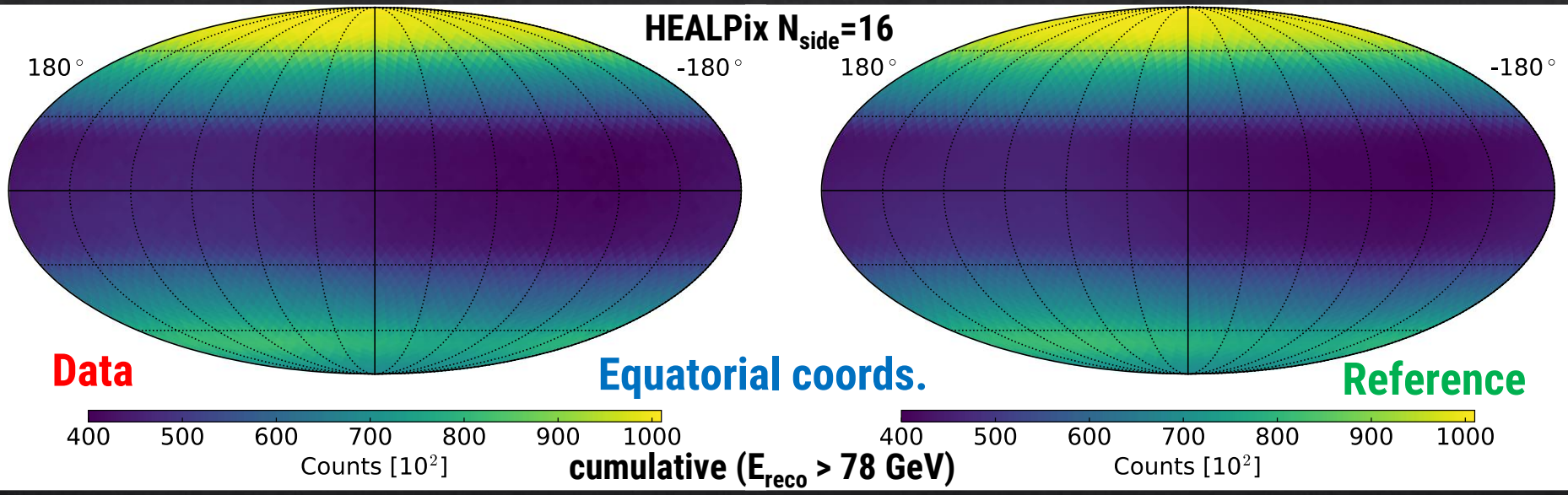

Data-driven method to estimate the **reference map**. Uses:

- Time-averaged event rate, R_{avg}
- Distribution of detected event directions in instrument coordinates, $P(\theta,\varphi)$

as empirical estimates of the detector's efficiency

+ average 100 realizations to beat down statistical noise

Fermi-LAT: Proton Anisotropy

[J. Vanderbroucke @ ICRC2019 & arXiv:1903.02905]

The **data map** is compared to the **reference map** and the relative intensity in **equatorial coordinates** is expanded in spherical harmonics using the HEALPix **anafast** algorithm

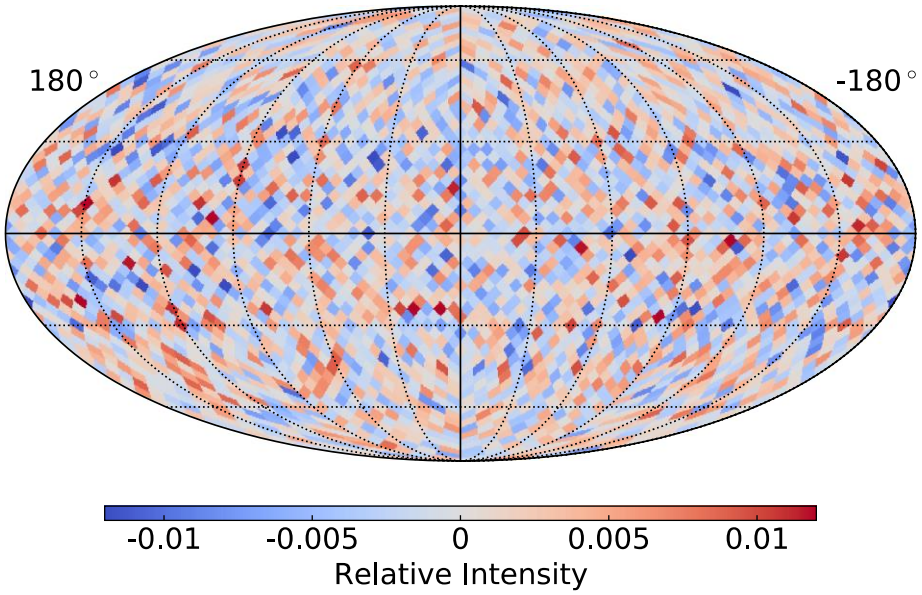

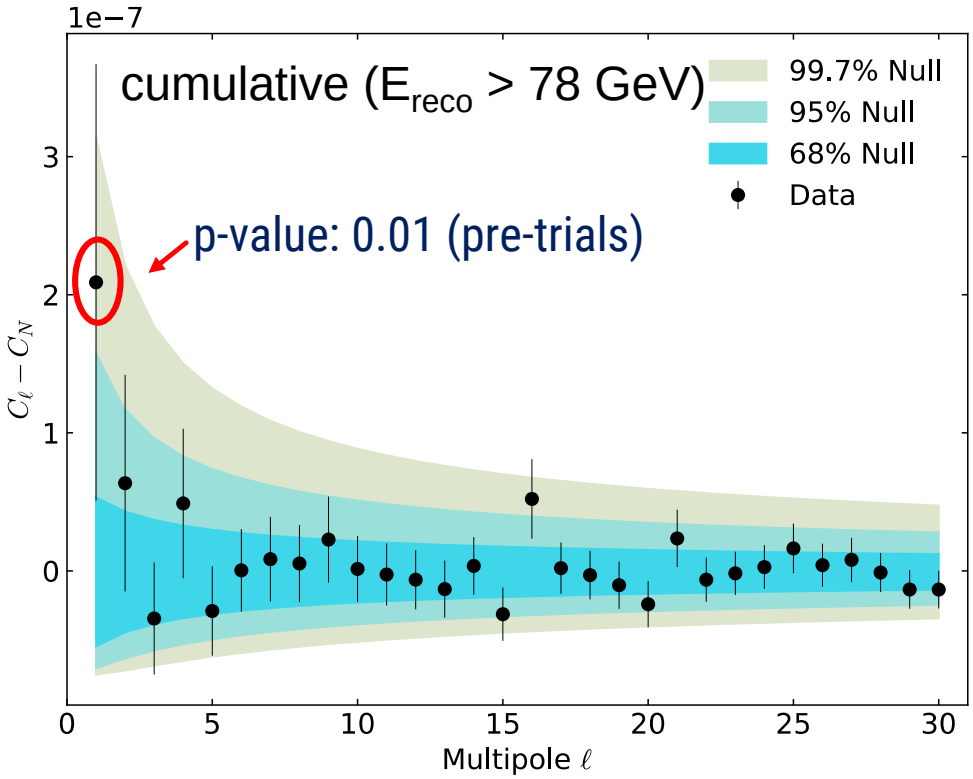

Fermi-LAT: Proton Anisotropy

[J. Vanderbroucke @ ICRC2019 & arXiv:1903.02905]

Dipole amplitude and **95% C.L. upper limits** are calculated for each cumulative bin in energy

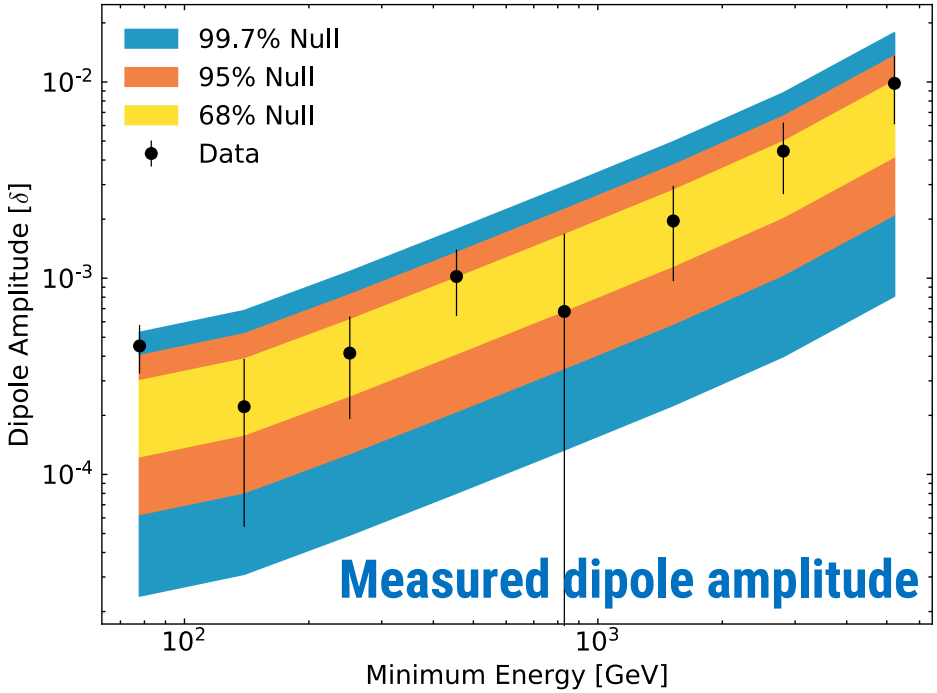

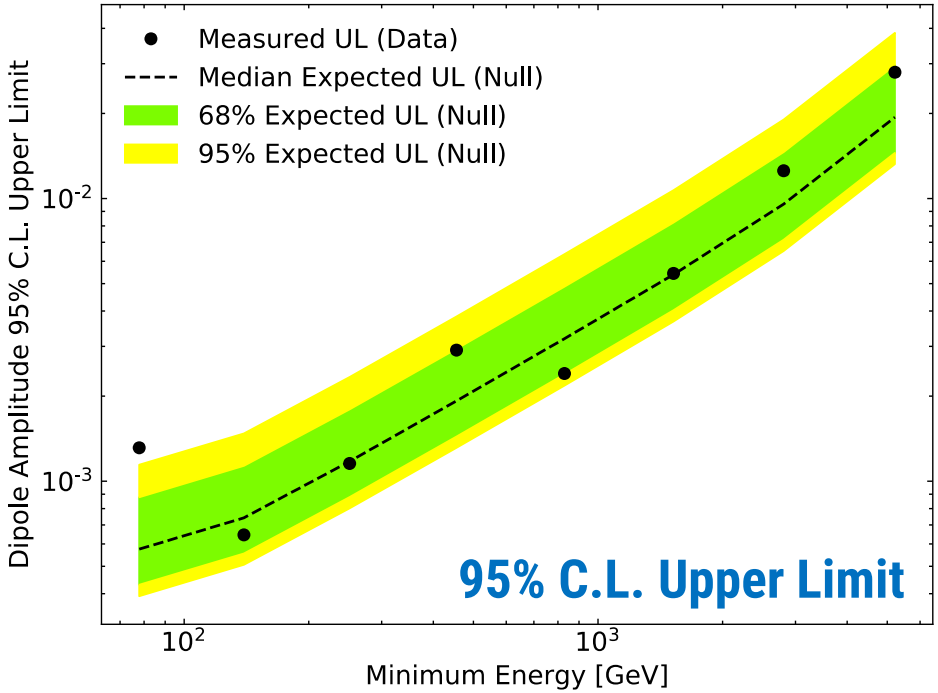

Dipole deviation for E_{rec} > 78 GeV range (δ_M=3.9×10^{-4}, δ_{UL}=1.3×10^{-3})

Rest of the energy cumulative bins are consistent with **isotropy**

CALET: Electron + Positron Anisotropy

CALET: [PoS(ICRC2019) 112]

The analysis is performed on the sample of **electron + positron events** collected by CALET in 1115 days (**~31 months**) from 2015 to 2018

Events are grouped into **5 cumulative ranges of energy** threshold equidistant in log scale between 125 GeV and 2 TeV

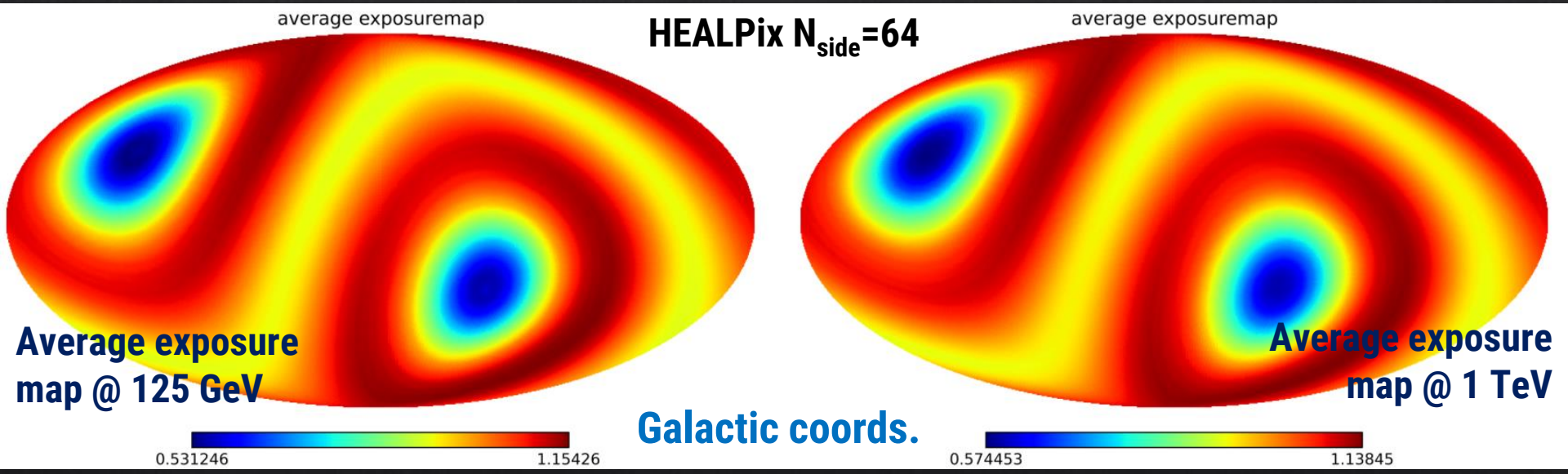

- **Exposure**: ISS orbit convoluted with the energy and direction dependent effective area
- **Events** are weighted relative to the average exposure and reconstruction efficiency

$$w_i = \frac{1}{A_i}\left(\frac{\sum_{events}\sum_{pixels} A(E, pixel)}{N_{events} N_{pixels})}\right)$$

CALET: Electron + Positron Anisotropy

CALET: [PoS(ICRC2019) 112]

The HEALPix **anafast** routines are used to perform a spherical harmonic decomposition of the event distribution on the sky in galactic coordinates

Results **in agreement with the expectation for an isotropic cosmic-ray flux**

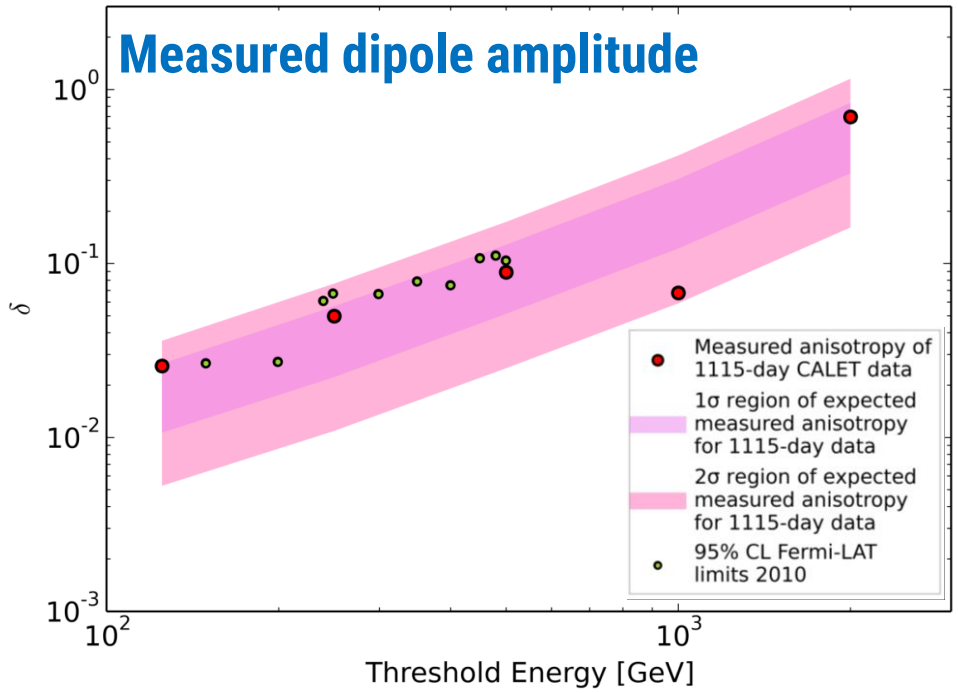

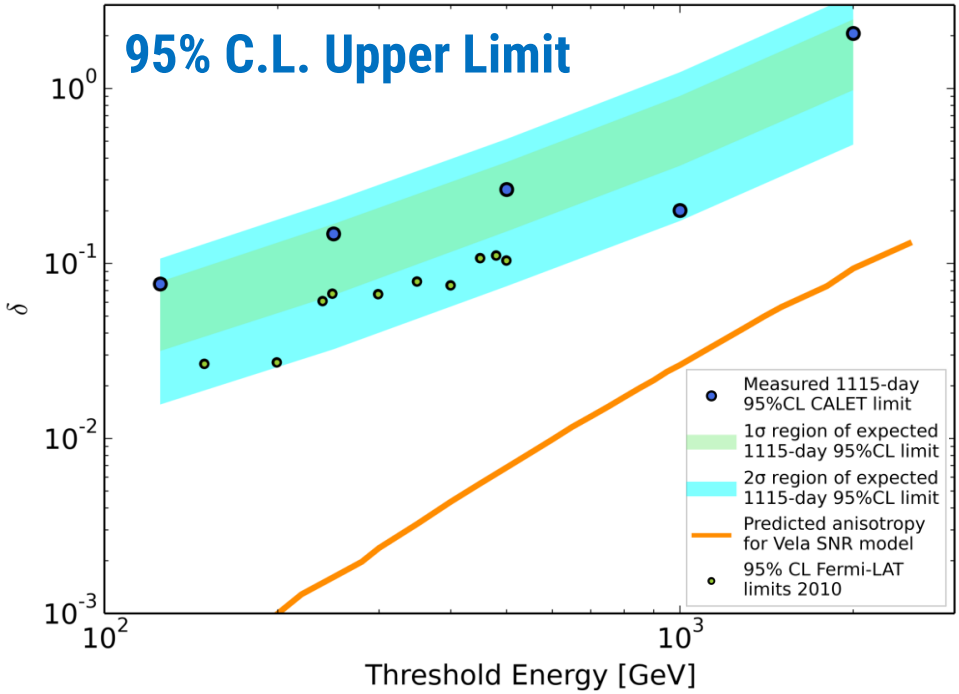

* Fermi-LAT independent energy ranges

The quadrupole and octupole moments were analyzed, as a check for the exposure correction. Results agree with the expectation from **isotropy**

Summary

Precision era in Cosmic Ray Physics has started thanks to space-based experiments

Observations **challenge** the standard paradigm of CRs origin and propagation. In particular, **indirect searches for DM** in CRs provide a window into fundamental physics

The study of the directionality of cosmic rays, i.e. the **anisotropy**, provides complementary information to the spectra and may help to understand the origin of these features

Currently, **AMS-02**, **Fermi-LAT**, **DAMPE** and **CALET** are providing precious information about GCRs physics and, in particular, about the **anisotropy**. Ongoing efforts to extend the energy range of the measurements and increase the overlap with ground-based detectors

Much fun to come in the next years!

Analysis of the Anisotropy

Measurement of the cosmic ray fluxes as function of the arrival direction in **Galactic Coordinates**

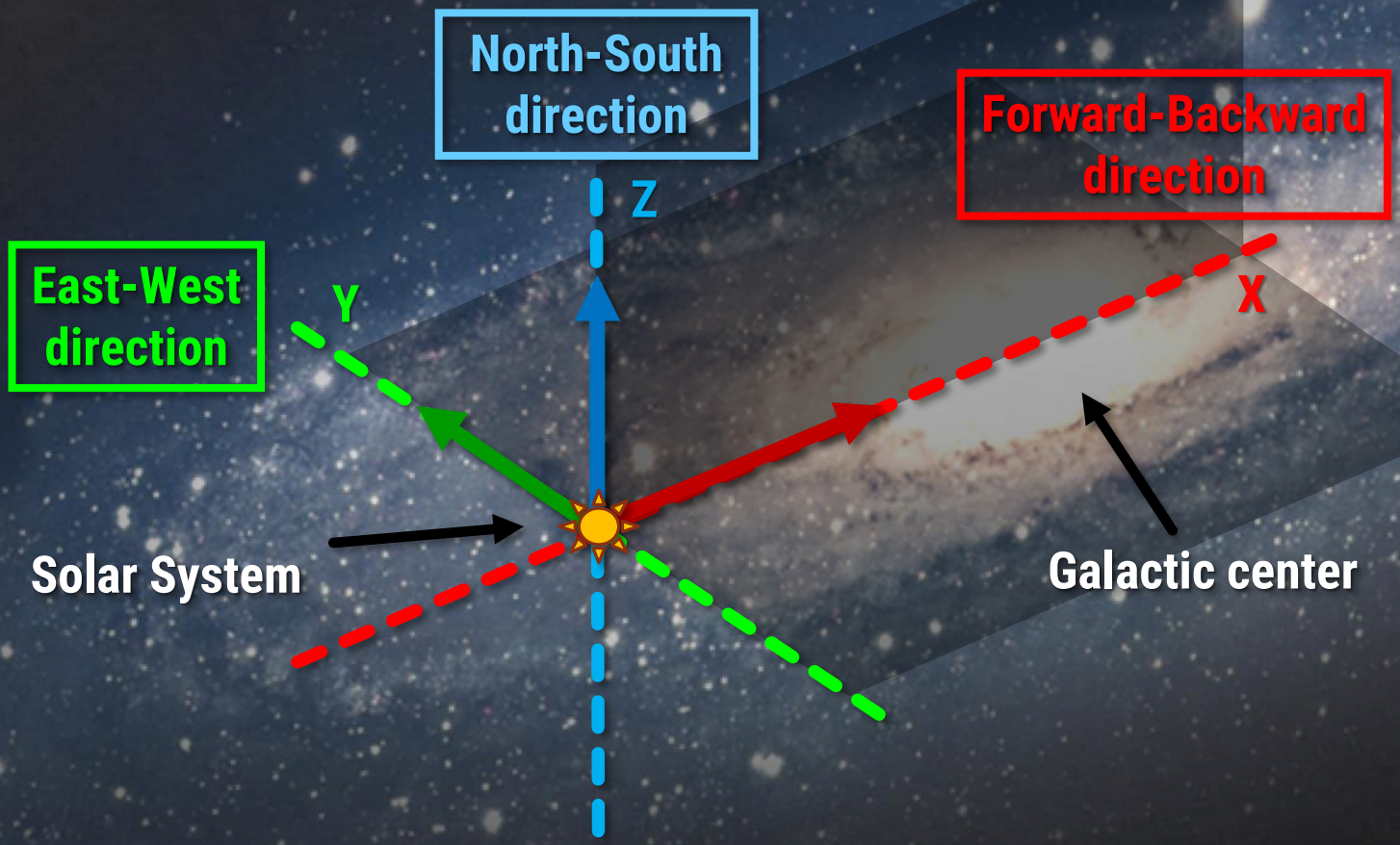

Spherical Harmonics Expansion of CR Fluxes

The directional dependence of the CR flux is described in terms of an expansion in **spherical harmonics**

$$\Phi(\theta,\varphi) = \Phi_0 \left(1 + \sum_{\ell=1} \sum_{m=-\ell}^{m=+\ell} a_{\ell m} Y_{\ell m}(\theta,\varphi) \right)$$

Multipolar components

Real spherical harmonics basis

Dipole anisotropy (ℓ=1)

Dipole amplitude

$$\delta = \frac{\Phi_{\max} - \Phi_{\min}}{\Phi_{\max} + \Phi_{\min}}$$

Dipole components

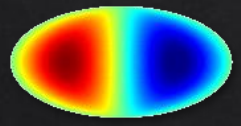

East-West

$$\rho_{\mathrm{EW}} = \sqrt{\frac{3}{4\pi}} a_{1-1}$$

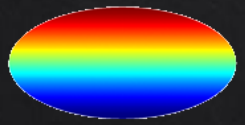

North-South

$$\rho_{\mathrm{NS}} = \sqrt{\frac{3}{4\pi}} a_{1+0}$$

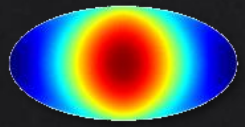

Forward-Backward

$$\rho_{\mathrm{FB}} = \sqrt{\frac{3}{4\pi}} a_{1+1}$$

$$\delta = \sqrt{\rho_{\mathrm{EW}}^2 + \rho_{\mathrm{NS}}^2 + \rho_{\mathrm{FB}}^2}$$

AMS-02: Positron Anisotropy

Dipole components - Galactic Coordinates

ρ_{EW}

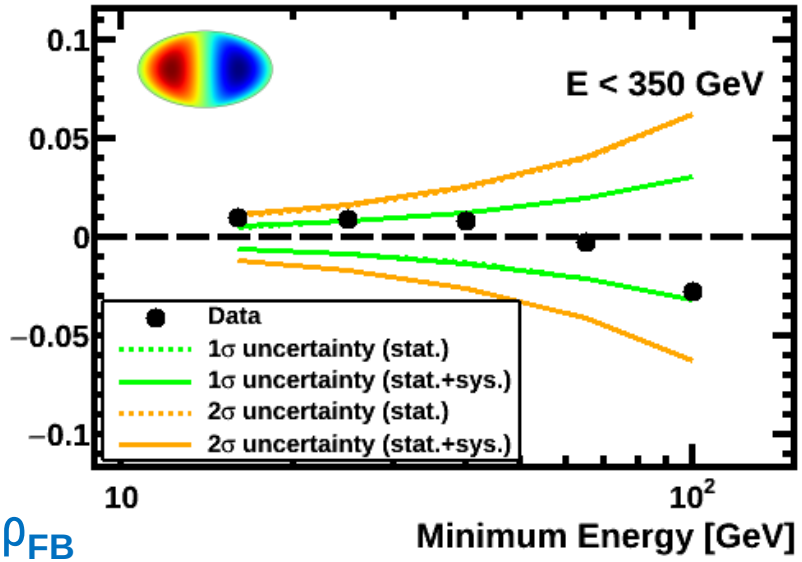

ρ_{NS}

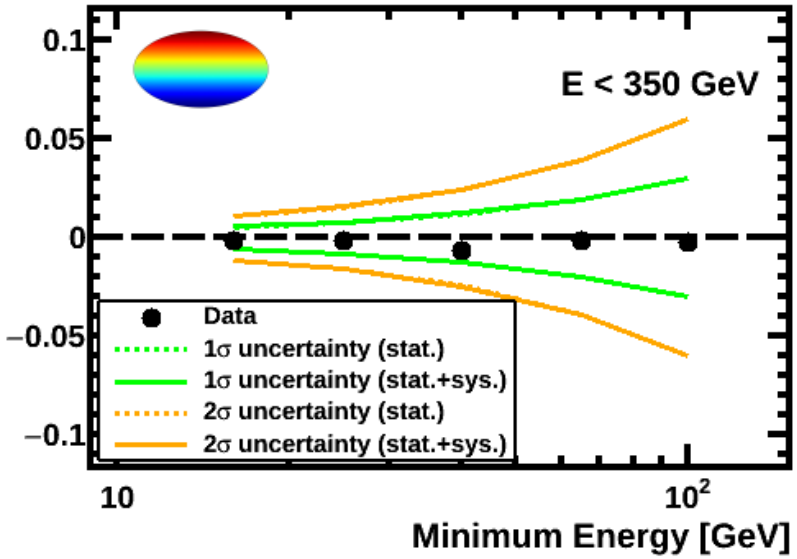

ρ_{FB}

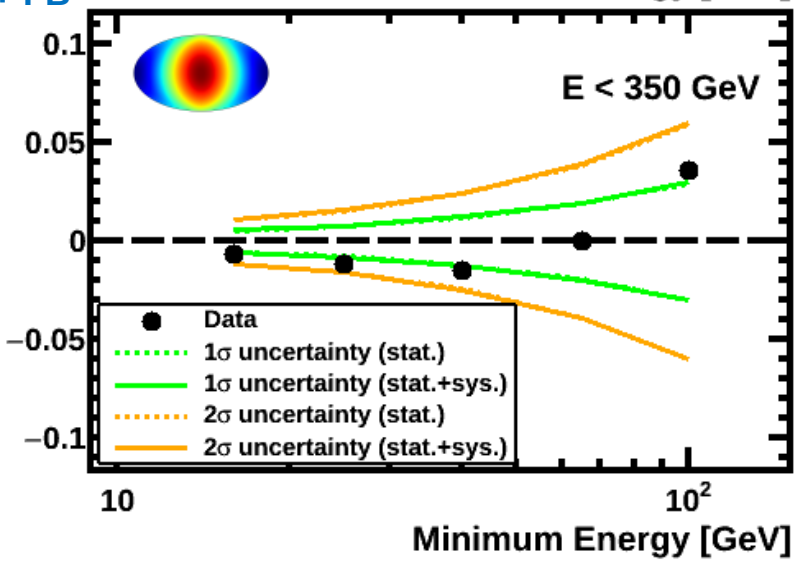

Results consistent with **isotropy** in all the **dipole components** and **energy ranges**

AMS-02: Electron Anisotropy

Dipole components - Galactic Coordinates

ρ_{EW}

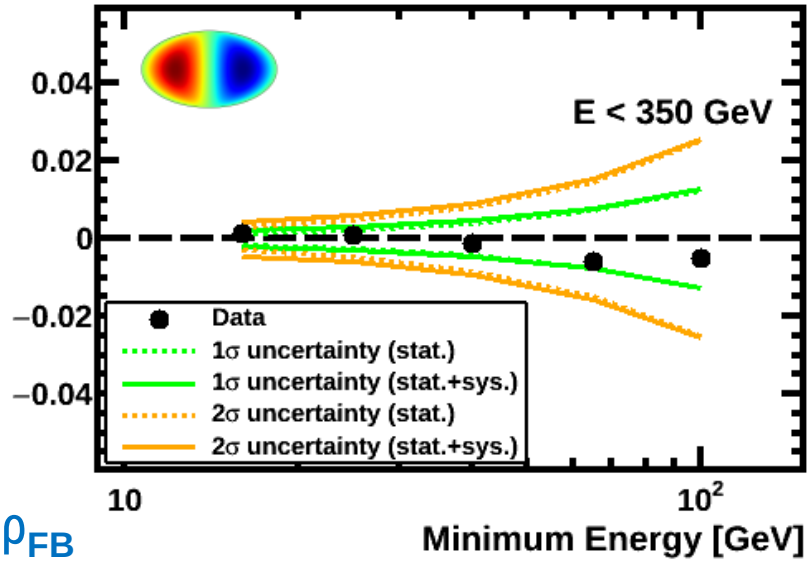

ρ_{NS}

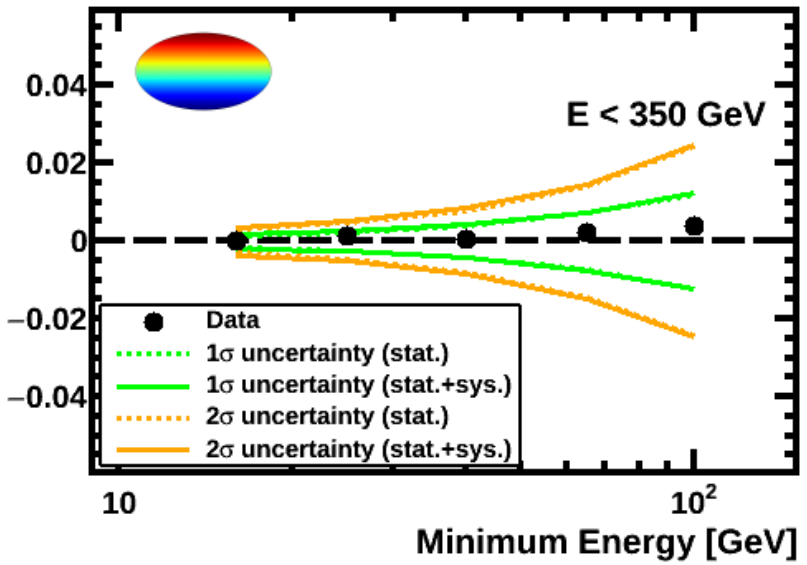

ρ_{FB}

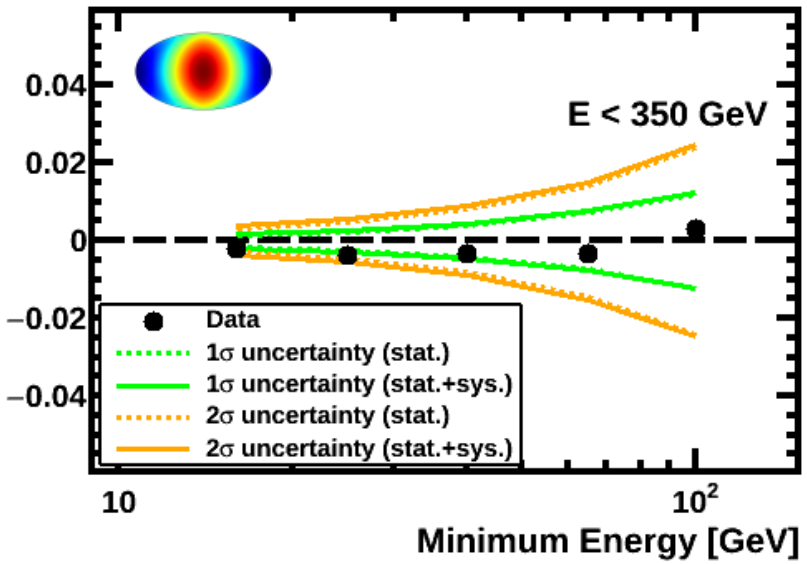

Results consistent with **isotropy** in all the **dipole components** and **energy ranges**

AMS-02: Proton Anisotropy

Dipole components - Galactic Coordinates

ρ_{EW}

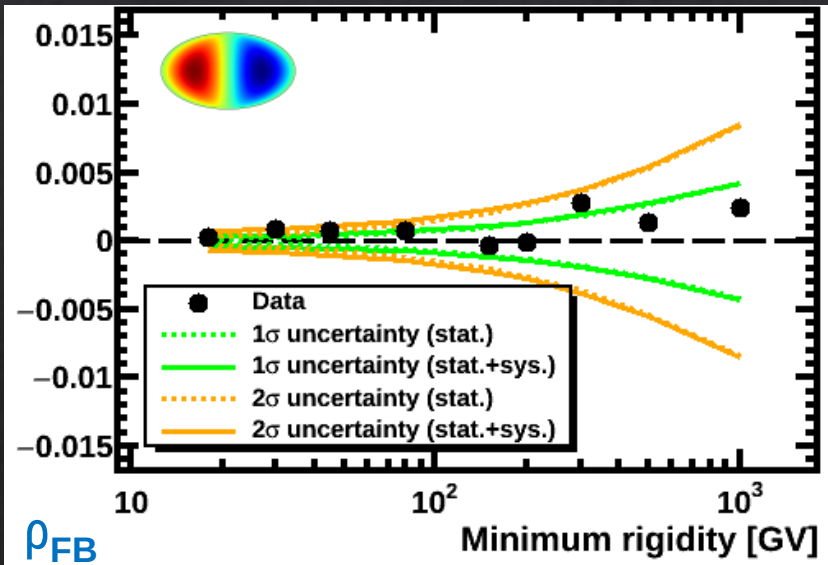

ρ_{NS}

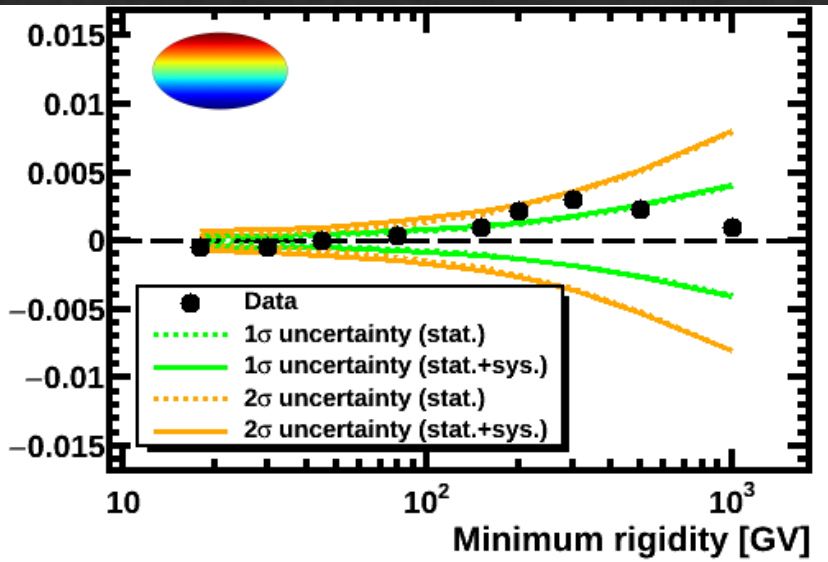

ρ_{FB}

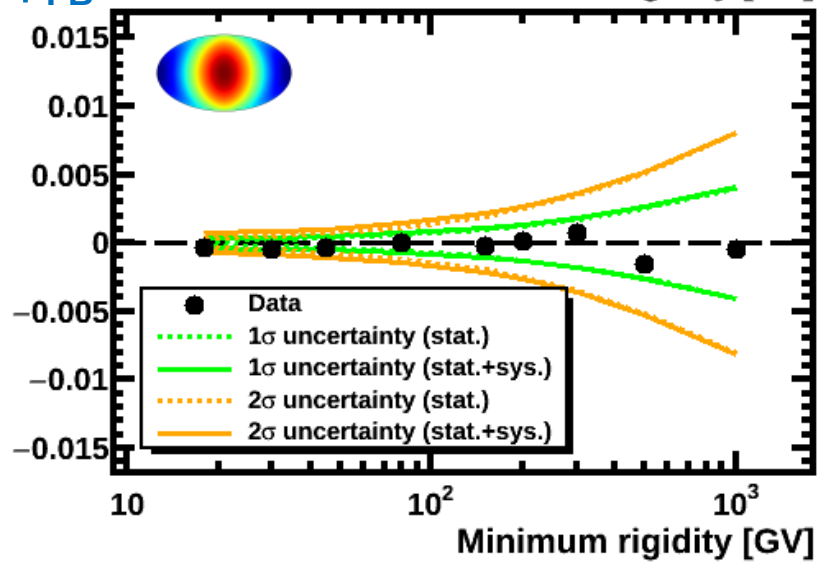

Results consistent with **isotropy** in all the **dipole components** and **rigidity ranges**

Fermi-LAT: Proton Anisotropy

Dipole components - Equatorial Coordinates

[J. Vanderbroucke @ ICRC2019 & arXiv:1903.02905]

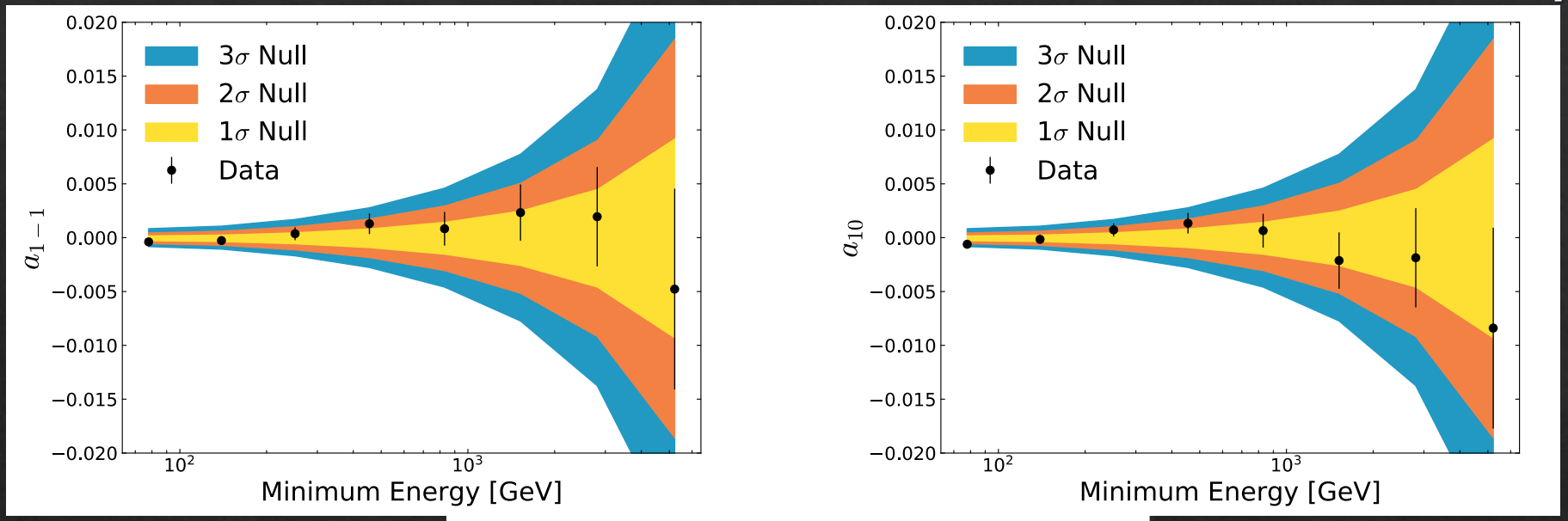

Fermi-LAT: Proton Anisotropy

Systematics – Geomagnetic cutoff

[J. Vanderbroucke @ ICRC2019 & arXiv:1903.02905]

$\theta < 60°$ 78-139 GeV $\theta < 45°$

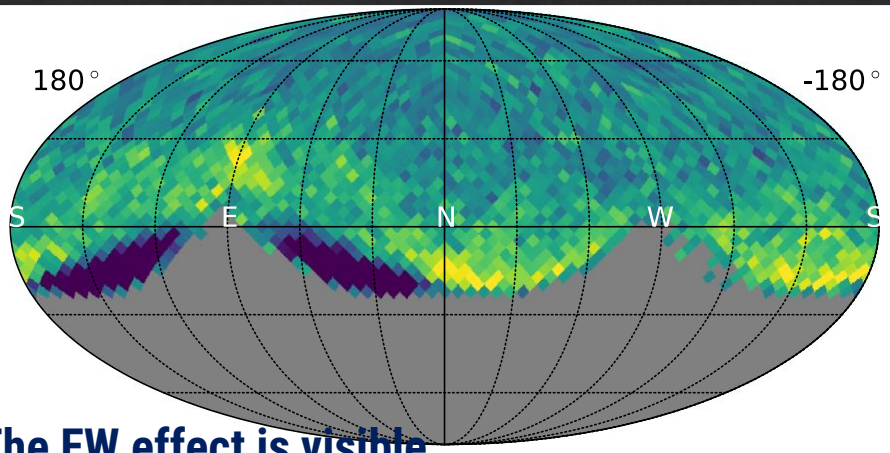

The EW effect is visible

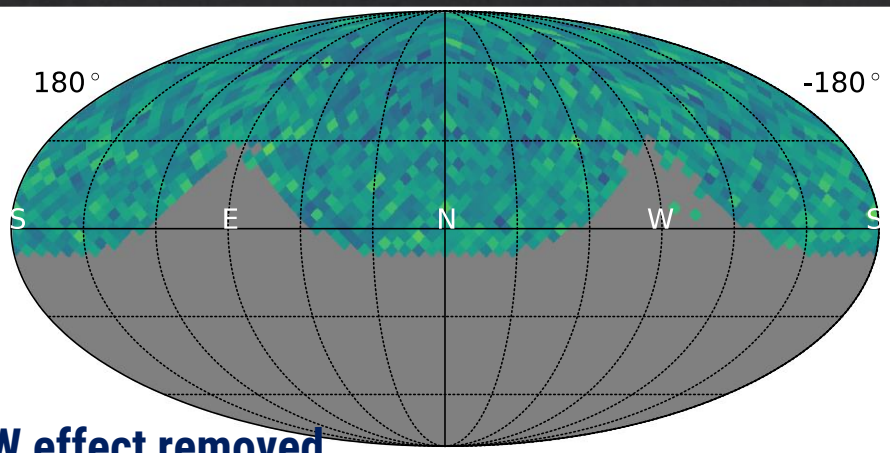

EW effect removed

altitude-azimuth coordinates

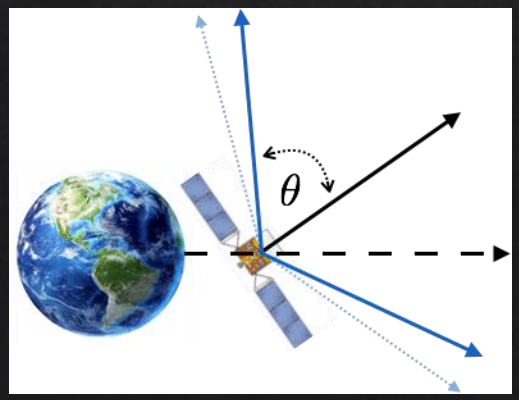

- By reducing the maximum off-axis angle θ, events close to the horizon are removed (higher geomagnetic deflections)
- Fermi-LAT uses $\theta < 45°$ below 139 GeV and $\theta < 50°$ above 139 GeV

Fermi-LAT: Proton Anisotropy

Systematics – PSF tail

[J. Vanderbroucke @ ICRC2019 & arXiv:1903.02905]

- Angular resolution for protons ~0.01° (68% angular containment)
- The tail of the PSF extends out to an angular error of 180° ⇒ protons entering from the bottom of the detector but reconstructed as downward-going particles
- Fermi-LAT : quadrupolar a_{2+0} exposure
- Events bad reconstructed pile up at the equatorial poles ⇒ a_{2+0} excess

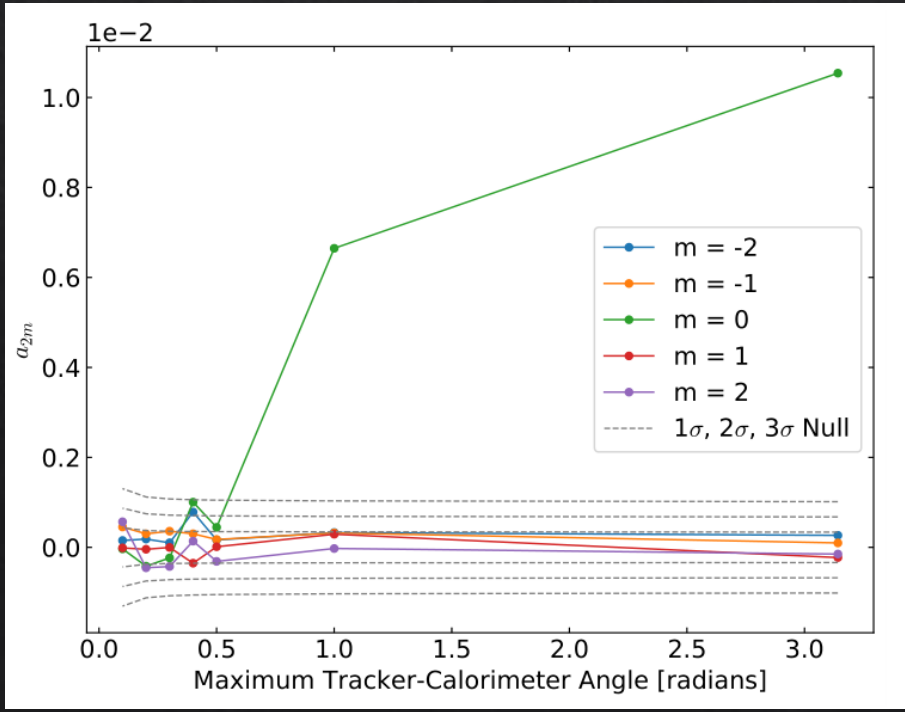

Use independent direction measurement by tracker and calorimeter (tracker-calorimeter angle) as a proxy for the quality of the reconstruction

The final cut of 0.2 is applied, where the a_{2+0} is consistent with isotropy

Fermi-LAT: Proton Anisotropy

Systematics – Event rate stability

[J. Vanderbroucke @ ICRC2019 & arXiv:1903.02905]

- The method to construct the reference map uses the time-averaged event rate over a year ⇒ not accounted rate variations may induce a spurious signal
- Fermi-LAT orbit covers regions of different geomagnetic cutoff ⇒ variations in the rate that might not be time-averaged

Relative variation of the rate vs McIlwain

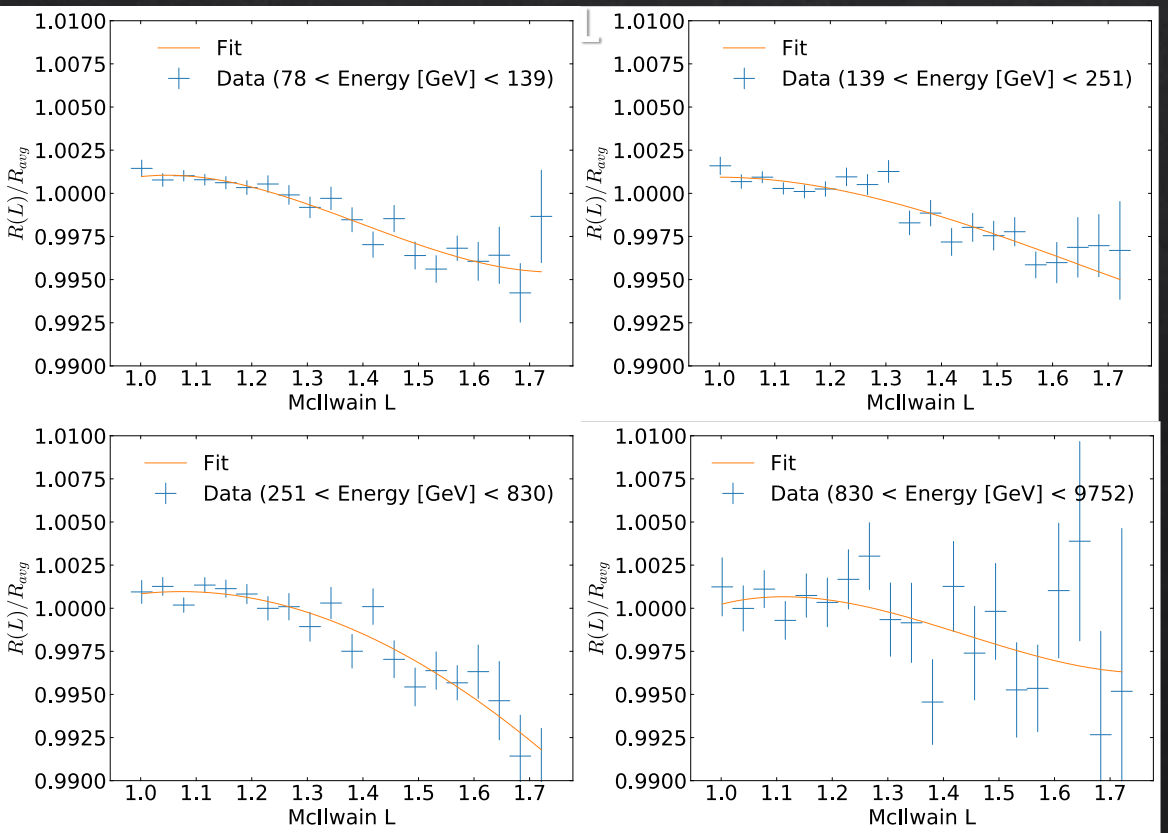

The observed event rate can vary by as much as 1% over the range of McIlwain L experienced by Fermi

A systematic 1σ dipole excess due to the McIlwain L-dependent event rate is expected

N.B.: The McIlwain L parameter describes the magnetic field lines: ~regions with the same geomagnetic cutoff